Science of the Total Environment 973 (2025) 179082

Contents lists available at ScienceDirect

Science of the Total Environment

journal homepage: www.elsevier.com/locate/scitotenv

Synergistic interaction of phosphate nanoparticles from fish by-products and phosphate-solubilizing bacterial consortium on maize growth and phosphorus cycling

Piera Quattrocelli [a,*], Clara Piccirillo [b], Eiko E. Kuramae [c,d], Robert C. Pullar [e], Laura Ercoli [a], Elisa Pellegrino [a]

[a] Institute of Crop Science, Scuola Superiore Sant'Anna, Piazza Martiri della Libertà 33, 56127 Pisa, Italy
[b] CNR NANOTEC Institute of Nanotechnology, via Monteroni, 73100 Lecce, Italy
[c] Department of Microbial Ecology, Netherlands Institute of Ecology (NIOO-KNAW), 6708 PB Wageningen, the Netherlands
[d] Ecology and Biodiversity Group, Department of Biology, Institute of Environmental Biology, Utrecht University, 3584 CH Utrecht, the Netherlands
[e] Department of Molecular Science and Nanosystems (DSMN), Università Ca' Foscari Venezia, Venezia Mestre, Venezia, VE 30172, Italy

HIGHLIGHTS

- Nanohydroxyapatite (nHA) plus seed coating (SC) improved maize productivity.
- Higher P-use efficiency with nHAs plus SC than nHAs alone or bacterial reinforce
- nHAs alone or combined with PSB strongly upregulated maize *PHT1* transporters.
- SC alone efficiently promoted bacterial establishment in the plant-soil system.
- Propionic acid release and P-solubilization by PSB with nHAs drive maize P uptake.

GRAPHICAL ABSTRACT

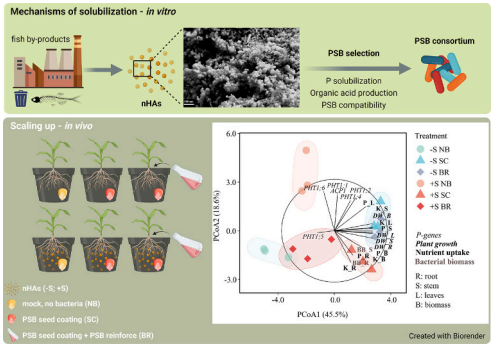

ARTICLE INFO

Editor: Charlotte Poschenrieder

Keywords:
Nanofertilizers
Food by-products
Microbial seed coating
P-use efficiency
Phosphate transporters
Inoculum establishment

ABSTRACT

Phosphate nanomaterials, such as hydroxyapatite/β-tricalcium nanoparticles (nHAs) derived from food industry by-products, offer a sustainable alternative to enhance P-use efficiency in agriculture. However, their limited solubility remains a challenge. This study first investigated the mechanisms of P solubilization of salmon and tuna bones (SnHAs and TnHAs) in fifteen strains of phosphate-solubilizing bacteria (PSB) by an *in vitro* system. Then, best-performing strains were assembled in a consortium and tested *in vivo* on maize. We hypothesized that combining nHAs and the PSB consortium inoculated as seed coating (SC) outperforms single treatments alone in promoting plant growth and P cycling, and ensures the establishment in plant-soil system without a bacterial reinforcement (BR) by an additional inoculum suspension. The synergistic effect of nHAs and PSB was proved, improving maize root (+22 %) and total plant biomass (+29 %), as well as P (+32 %) and K (66 %) uptake compared to single treatments. With nHAs and SC, P-use efficiency and recovery increased by 25 % and three-fold, respectively, compared to nHAs alone or with bacterial reinforcement. Consistently, root and substrate

* Corresponding author.
E-mail address: piera.quattrocelli@santannapisa.it (P. Quattrocelli).

https://doi.org/10.1016/j.scitotenv.2025.179082
Received 9 December 2024; Received in revised form 6 March 2025; Accepted 6 March 2025
Available online 18 March 2025

bacterial biomass were associated with nHAs plus SC, while nHAs alone or with PSB upregulated *PHT1;1* and *PHT1;2* transporter genes in maize. Finally, linking the *in vitro* and *in vivo* system, we demonstrated that propionic acid production and P-solubilization efficiency of PSB co-applied with nHAs are key drivers of maize growth and P uptake. Our findings indicated that co-applying nHAs and PSB through SC offers a sustainable strategy to improve maize P-use efficiency.

1. Introduction

Phosphorus (P) is essential for crop development, supporting plant growth from early stages to vegetative and reproductive phases (de Bang et al., 2021; Zhang et al., 2023). It plays a fundamental role in root development, aboveground biomass accumulation, seeds formation, and grain quality enhancement (Mollier and Pellerin, 1999; Wang et al., 2023). Plant availability of soil P is limited due to several factors, including high soil pH, immobilization onto clay particles, precipitation with cations (*e.g.*, Ca, Al, Fe), and binding in metal complexes (Shen et al., 2011; Roberts and Johnston, 2015; Azam et al., 2019). Traditionally, mineral P fertilizer production has relied on finite rock phosphate reserves, with 50 % projected to be depleted by 2100 (van Vuuren et al., 2010). The increasing demand for P fertilizers, along with the need to maintain and improve soil P status, has heightened the urgency of improving P use efficiency. However, P recovery rarely exceeds 30 % of the applied P within the first year, and often remains within the 10–15 % range (Hedley and McLaughlin, 2005; Roberts and Johnston, 2015; Liu and Lal, 2015). Nevertheless, P-recovery efficiency varies significantly, as it depends on multiple factors, including soil properties, the solubility of newly formed P compounds, and plant species (Sonmez and Pierzynski, 2017). Generally, P is applied as phosphate salts, which are easily leached off (Sharpley et al., 2001), or as solid formulations with large particle sizes and low soil mobility (Reynolds and Davies, 2001). As a result, P fertilizer application has led to substantial variability in topsoil availability worldwide, contributing to environmental concerns (Swaney and Howarth, 2019; Panagos et al., 2022). Excessive soil P accumulation has caused P leaching and, therefore, long-term surface water degradation, promoting algal blooms and other symptoms of eutrophication (Schindler et al., 1974; Carpenter, 2005; Dupas et al., 2015). Additionally, immobilized P can be lost through water soil erosion and transported by sediments, significantly reducing P-recovery efficiency and, in some cases, contributing to P runoff into water bodies (Carpenter and Bennett, 2011). Given these challenges, it is essential to develop efficient alternatives to mineral P fertilizers, while reducing reliance on non-renewable P sources and mitigating their economic and environmental consequences (Sharpley et al., 2001; Herrera-Estrella and López-Arredondo, 2016).

Emerging nanotechnologies offer promising strategies to improve P use efficiency (Gogos et al., 2012; Hazarika et al., 2022; Liu and Lal, 2015). Recently, hydroxyapatite-based nanoparticles (nHAs) have gained attention for their small particle size, high surface area, and gradual P release in soil (Montalvo et al., 2015; Xiong et al., 2018a). Hydroxyapatite (HA, $Ca_{10}(PO_4)_6(OH)_2$) is a naturally occurring biocompatible phosphate and the primary inorganic component of some food industry by-products and waste materials, such animal and fish bones (Piccirillo et al., 2014; Abdelmigid et al., 2022; Pilotto et al., 2024). After heating, HA often co-exists with β-tricalcium phosphate (β-TCP, $Ca_3(PO_4)_2$), structurally similar but more soluble than HA. Nevertheless, although nHAs have been proposed due to their slow release and their potential ability to directly enter in plant cells (Montalvo et al., 2015), the low solubility of HA may limit their effectiveness for crop P uptake (Larsen, 1966; Nair et al., 2010; Liu and Lal, 2015).

So far, under greenhouse conditions, synthetic nHAs have been reported to increase soybean grain yield and plant biomass by 21 % and 30 %, respectively, compared to mineral fertilizer with the same P content (Liu and Lal, 2014). However, the increases were not statistically significant. Substantial improvements in soybean grain yield and root biomass, from five- to 57-fold increases, were observed compared to controls fertilized without P. Similarly, in controlled environments, synthetic nHAs at high rates (50 and 150 mg of P per kg of soil) increased maize leaf biomass by 78 % and root and leaf P accumulation by 70 % and 183 %, respectively, compared to unfertilized controls (Jia et al., 2022). Furthermore, synthetic nHAs enhanced wheat shoot dry weight and P uptake, particularly in acidic soils, compared to both unfertilized control and bulk HA (Montalvo et al., 2015). Additionally, three different synthetic nHAs with varying surface charges were tested on sunflower in P-deficient soils receiving basal mineral fertilization (Xiong et al., 2018b). Negatively charged nHAs outperformed triple superphosphate (TSP), rock phosphate and untreated controls in terms of plant biomass, whereas positively and neutral charged nHAs exhibited similar performance to TSP. Moreover, neutral and negatively charged nHAs led to the highest shoot P uptake. Unlike TSP, which exhibited a sharp decline in soil P release over time, nHAs maintained a more constant dissolution rate, which improved their effectiveness (Xiong et al., 2018a,b). In addition, nHAs derived from fish bones promoted maize seedling growth and total dry mass by 50 % to four-fold (Carella et al., 2021). This improvement was not correlated with the P dissolution rate, as even the less soluble nHAs performed well as fertilizer. These findings suggest that other factors beyond solubility in water play a crucial role in P availability in soil and fertilizer use efficiency. Other key factors may include soil interactions such as microbial activity and soil organic matter.

Under field conditions, applications of synthetic nHAs at increasing rates (40–80 kg P_2O_5 ha^{-1}, equivalent to 17 and 35 kg P ha^{-1}), had no significant effect on wheat grain yield or P uptake in grains and whole plants compared to the diammonium phosphate (DAP, 80 kg P_2O_5 ha^{-1}) (Taskin and Gunes, 2023). Therefore, while previous in controlled studies support nHAs as a viable alternative to conventional fertilizers, further research is needed to fully assess their effectiveness and to ameliorate P solubilization (Zhu et al., 2023).

Phosphate-solubilizing bacteria (PSB) have been recently proposed for their ability to enhance P solubility from both synthetic and biogenic nHAs (Santana et al., 2019; Monroy Miguel et al., 2020; Kooshki and Haghighi, 2024). These soil microbes thrive in the rhizosphere or even colonize the endosphere of plants (Emami et al., 2020), and play a crucial role in plant P acquisition by converting insoluble P compounds into plant-available forms (Alori et al., 2017; Raymond et al., 2021). One of the primary mechanisms though which PSB enhance P solubility is the release of low-molecular-weight organic acids (OAs), which improves P mobility in soils and its availability to plants (Farhat et al., 2015; Manzoor et al., 2017; C. Li et al., 2021; X.L. Li et al., 2021). The production of OAs lowers soil pH, thereby promoting the solubilization of calcium phosphates, including HA (Rodriguez and Fraga, 1999). However, few studies have investigated the interaction between PSB and nHAs, and they suggested that PSB strain selection is crucial for efficient P solubilization (Santana et al., 2019; Monroy Miguel et al., 2020; Kooshki and Haghighi, 2024; Pilotto et al., 2024). Moreover, the type of applied nHAs may influence the efficiency of such interactions. For instance, among 17 bacterial strains, only two demonstrated P dissolution levels comparable to tricalcium phosphate (TCP) (used as reference in PSB studies) within just eight days post-inoculation (Santana et al., 2019). Similarly, only 12 out of 43 bacterial strains efficiently solubilized TCP *in vitro* (up to 54 %) after 20 days, whereas with nHAs, six strains achieved P solubilization rates up to 73 % after five days (Monroy

Miguel et al., 2020). All bacteria secreted citric acid and other OAs (*i.e.*, succinic, lactic, propionic and malic acids), whereas none produced oxalic, phosphoric, gluconic, malonic or maleic acids. These findings are consistent with the results of Wang et al. (2016), who reported that nHA dissolution efficiency followed this order: citric > oxalic > acetic acid. When applied in soil, nHAs derived from chicken bones, either alone or in combination with *Pseudomonas alloputida*, promoted root and total dry weight of barley and increased soil P availability, achieving values comparable to the sole application of *P. alloputida* under unfertilized controls (Pilotto et al., 2024). Despite a 16 % higher soil P availability in nHA and PSB treated soils, compared to the sole application of nHAs, no significant differences in plant P uptake were observed. Conversely, when applying two doses of nHAs derived from animal bones with *Pseudomonas putida*, tomato plant exhibited enhanced fruit yield compared to unfertilized controls, regardless bacterial inoculation (Kooshki and Haghighi, 2024). Furthermore, PSB co-application resulted in additional improvements in shoot and root biomass compared to nHAs alone. Similarly, when maize was treated with nano-rock phosphate and *Bacillus cereus*, greater root biomass (38 %), grain yield (14 %), shoot and grain P accumulation (26 % and 9 %) and P-use efficiency (18 %) were reported compared to not-inoculated controls (Yasmeen et al., 2022). These results were attributed to decreases in rhizosphere pH, which enhanced bacterial P solubilization and increased P desorption from soil particles. Given these findings, there is a knowledge gap on the mechanisms underlying the efficacy of the combined use of nHAs and PSB.

Phosphate-solubilizing bacteria can be applied either as a single strain or as consortia. Studies indicate that PSB consortia exhibit greater resilience and adaptability under fluctuating environmental conditions (Haskett et al., 2021; Khan, 2022). These advantages are associated with synergistic interactions between different PSB strains, allowing them to perform complementary functions, such as enhanced nutrient solubilization, pH modulation, and increased microbial stability in the soil (Kumar et al., 2016; Hu et al., 2021). For example, when *Pseudomonas spp.* were applied as consortia at increasing species richness, they exhibited enhanced auxin production, P solubilization, and C metabolism compared to single strains (Hu et al., 2021). Additionally, when tested on tomatoes, microbial consortia significantly increased aboveground biomass, N, P, K content in plant tissues, and ensured stable *Pseudomonas* presence in the rhizosphere.

To improve the establishment and survival of PSB inoculants, seed coating (SC) has been explored as a promising delivery method. It facilitates the direct introduction of inoculated microbes to plant roots (Cortés-Rojas et al., 2021; Ma, 2019). Additionally, SC could enhance a closer association between PSB and insoluble P sources, further improving P solubilization (Raymond et al., 2021). However, one limitation of SC-based inoculation is the relatively low number of bacterial cells attached to the seed surface, which may reduce the effectiveness of inoculation (Bashan et al., 2014). Thus, further research is needed on PSB consortia rather than single strains, as well as on the optimization of SC and inoculation methods to enhance P solubilization efficiency and ensure the soil survival and activity of PSB inoculants.

Therefore, this study aims to uncover for the first time the mechanisms through which a consortium of PSB enhances the solubilization of nHAs synthesized from fish by-products. We hypothesized that: (i) combining nHAs and a PSB consortium as SC provides greater benefits to plant growth, P uptake, and P-use efficiency than single treatments; (ii) SC promotes the establishment and growth of PSB in plant-soil system without the need for a simultaneous PSB re-inoculation. Initially, nHAs with varying solubilities were synthesized from salmon and tuna bones and physico-chemically characterized. An *in vitro* bottom-up approach was employed to identify the most effective PSB strains across different substrates and pH conditions, and focusing on OAs production as mechanism of solubilization. Then, after assessing IAA production, N fixation, and compatibility among strains, a multifunctional PSB consortium was assembled. This system was scaled-up to an *in vivo* experiment with maize (*Zea mays* L.) as a model plant, evaluating the effects of PSB SC alone and in combination with an additional PSB inoculum reinforcement, and its interaction with nHA on plant. Maize growth, P and K uptake, and P-use efficiency as a proxy for environmental sustainability, resource conservation and pollution mitigation, were used for the assessment. Phosphorus plant uptake was also investigated by analyzing the expression of six P-related genes, and total bacterial biomass was quantified as an indicator of bacterial soil enrichment and root colonization. Finally, we examined the relationship between P-solubilization efficiency and OA production of the PSB consortium in interaction with nHAs and plant parameters to identify the key traits responsible for plant functional changes.

2. Materials and methods

2.1. Salmon and tuna nHAs

Salmon bones were sourced from a local supermarket in Lecce (Italy), while tuna bones were provided by Mare Aperto S.p.A. (Genova, Italy). The dried bones were calcined in air at 700 °C in a Naberthem furnace (Nabertherm GmbH, Lilienthal, Germany) with a heating rate of 5 °C per minute for a duration of 1 h. The calcined bones were then manually crushed into a powder, and further refined by ball milling in isopropyl alcohol to achieve a uniform particle size, producing salmon and tuna nHAs (SnHAs and TnHAs, respectively) (Teixeira et al., 2017). The phase composition, determined by X-ray diffraction (XRD), showed that SnHAs had a ratio of β-TCP:HA of 45 %:55 % (w/w), while TnHAs were composed of 98–99 % pure HA (Fig. S1a), which is less soluble than β-TCP (Dorozhkin and Epple, 2002). FTIR spectra for SnHAs and TnHAs showed similar features, namely the presence of peaks attributed to phosphate and carbonate groups, and HA (Fig. S1b). SnHAs also showed an additional peak corresponding to β-TCP (Ebrahimi et al., 2017). The Zeta potential (ζ) of SnHAs was −34.7 mV (± 0.2 mV) (Fig. S1c), indicating sufficient repulsive force to prevent particle agglomeration and flocculation. The ζ of TnHAs was below the threshold of agglomeration (−15.3 ± 0.6 mV) (Fig. S1c), indicating instability in the solution (Mahbubul et al., 2019). The scanning electron microscopy (SEM) micrographs of SnHAs indicated spherical particles (Ø < 50 nm) (Fig. S1d, e), while particles with an elongated shape were observed for TnHAs (200–400 nm in length and 30–50 nm in width) (Fig. S1f,g respectively). The P concentration, spectrophotometrically determined (Piccirillo et al., 2014), was 18.4 % for SnHAs, 16.6 % for TnHAs, and 17.5 % for β-TCP. β-TCP was used as reference phosphate in the following *in vitro* screenings. Details about the synthesis and characterization of SnHAs and TnHAs are reported in Supplementary Materials and methods 1.

2.2. In vitro characterization and phosphate solubilization efficiency of PSB strains

Fifteen bacterial strains, previously identified as capable of solubilizing β-TCP or classified as potential PSB, were selected from earlier studies (*e.g.*, Pérez-Rodriguez et al., 2020; Sessitsch et al., 2005). The identities, DSMZ numbers, and internal codes of these strains are provided in Table 1 (for references see Table S1). All selected bacterial strains are classified as biologically safe (Risk Group 1) according to the German Federal Institute for Occupational Safety and Health. The *in vitro* qualitative screening allowed selecting the six best-performing PSB strains (PG0319, PG1211, PR0393, PC1218, PT0405, PP0616) and one mild performer (PF0520). Details about the *in vitro* qualitative screening on six different inorganic P sources with varying solubility, *i.e.*, β-TCP, SnHAs, TnHAs, mineral nHAs (MnHAs), $AlPO_4^-$, and $FePO_4^-$, are given in Supplementary Materials and methods 2. Additionally, these strains were IAA producers (Fig. 1b,c) (Cumpa-Velásquez et al., 2021), and N_2 fixers, except for PT0405 (Fig. 1d,e) (Batista et al., 2021). Moreover, these strains grew optimally on plates amended with CMC, as indicated by the EI values (Fig. S2). Information on the methodologies for

Table 1
Identities and codes of the phosphate-solubilizing bacterial (PSB) strains used in the study. See Table S1 for references.

PSB strain identity	DSMZ number[a]	Internal code[b]
Cellulosimicrobium cellulans	DSM 20106	CC1
Cellulosimicrobium cellulans	DSM 46031	CC2
Cellulosimicrobium terreum	DSM 18665	CT1006
Pantoea eucalypti	DSM 23077	PE1109
Paraburkholderia terricola	DSM 17221	PT0405
Paraburkholderia phytofirmans	DSM 17436	PP0616
Paraburkholderia phytofirmans	DSM 103130	PP0220
Priestia megaterium	DSM 3228	BM0204
Pseudomonas corrugata	DSM 7228	PC1218
Pseudomonas fluorescens	DSM 289	PF0520
Pseudomonas graminis	DSM 100941	PG0319
Pseudomonas graminis	DSM 11363	PG1211
Pseudomonas koreensis	DSM 16610	PK0810
Pseudomonas moorei	DSM 12647	PM12647
Pseudomonas rhodesiae	DSM 7527	PR0393

[a] DSMZ: German Collection of Microorganisms and Cell Cultures GmbH (https://www.dsmz.de).
[b] Internal code: the code used in the study.

characterizing strain properties are provided in Supplementary Materials and methods 3.

The seven selected PSB strains were used for a quantitative *in vitro* analysis of P solubilization over time under acidic (pH: 5.5) and alkaline conditions (pH: 7.5). Three different P sources were chosen to represent a gradient of solubility: β-TCP (high solubility), SnHAs (medium solubility) and TnHAs (low solubility), with β-TCP included for comparison. The PSB strains were grown as described in Supplementary Materials and methods S2. A 100 μL aliquot of overnight bacterial culture (OD600nm = 0.1) was inoculated into 100 mL flasks containing 50 mL of liquid NBRIP, adjusted pH of 5.5 and 7.5. Uninoculated flasks served as negative control, and each treatment was performed in quadruplicate. The cultures were incubated in a rotary shaker at 28 °C at 140 rpm in dark conditions. Samples of 1.5 mL were collected from each flask at intervals of 0, 3, 5 and 7 days (designed as T0, T3, T5, and T7, respectively) for quantitative P analysis. The collected samples were centrifuged at 10,000 rpm for 10 min, and the P content in the supernatant was measured using a spectrophotometer (Infinity Pro200, TECAN) at 400 nm, calibrated against a standard KH_2PO_4 curve, and analyzed with the Merck Spectroquant P reagent kit (Piccirillo et al., 2014). To calculate the percentage (%) of solubilized P, the total P content (w/w)

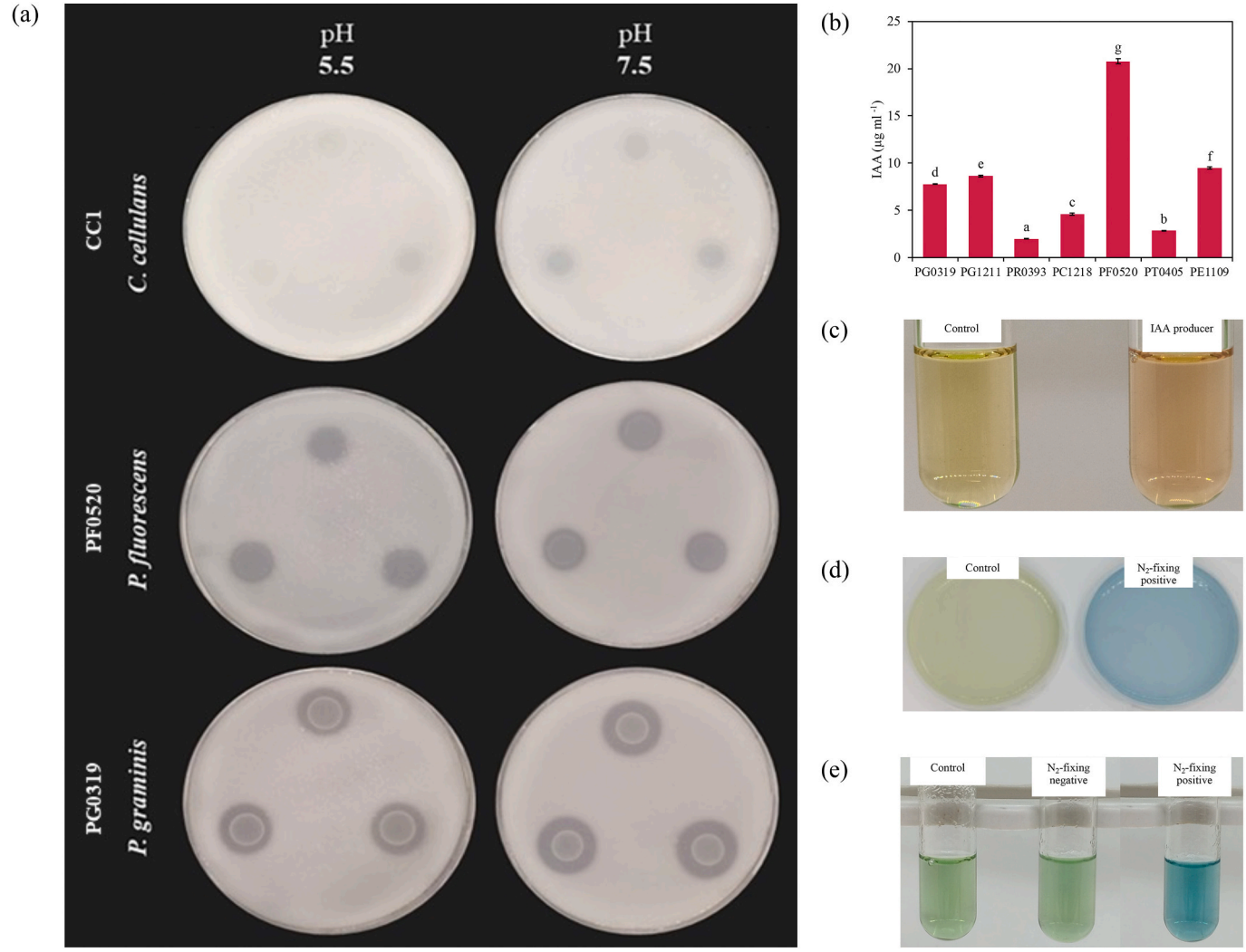

Fig. 1. Examples of the phosphate-solubilizing activity on tricalcium phosphate by weak (CC1, *Cellulosimicrobium cellulans*), mild (PF0510, *Pseudomonas fluorescens*), and strong (PG0319, *Pseudomonas graminis*) phosphate-solubilizing bacteria (PSB) screened under acidic (left) and alkaline pH (right); (b) indole acetic acid (IAA) production by PSB. Data are mean ± SE. Different letters represent significant differences among strains, according to one-way ANOVA and *post hoc* Tukey-B test ($P < 0.001$); (c) examples of IAA producing strains and controls; (d) biological N_2-fixing activity by PSB on solid and (e) on semi-solid New Fabio Pedrosa medium. The control represents the non-inoculated media. See Table 1 for PSB identities.

was determined in β-TCP, SnHAs and TnHAs. See Materials and methods S1 for details. At each time point, pH changes in the medium were also measured to monitor potential acidification, which may indicate organic acid production by PSB strains (Chen et al., 2006).

2.3. Characterization of OAs secreted by PSB

At the end of the *in vitro* quantitative screening (T7), samples were harvested and filtered (Ø = 0.2 μm) to investigate the OA production by PSB strains within each substrate and pH conditions (three replicates for each strain, substrate and pH). The detection and quantification of targeted OAs (*i.e.*, acetic, tartaric, oxalic, malic, fumaric, succinic, gluconic and propionic acids) were carried out on the seven selected PSB strains by Ultra Performance Liquid Chromatography-Mass Spectrometry (UPLC-MS) (Feng et al., 2010) equipped with Waters H-Class quaternary pump, with an autosampler, and coupled with XEVO TQD detector (Waters, USA). Isocratic elution was performed using a Waters Aquity UPLC HSS T3 column (2.1 mm × 50 mm, Waters, USA), with the mobile phase consisting of ammonia 0.05 % in MilliQ water, with a flow rate of 0.3 mL min^{-1}, and maintained at 45 °C. Samples (30 μL) were directly injected into the column, and OAs were identified by retention time and mass fragments of OAs analytical standards (Chebios, Italy).

2.4. In vivo experimental system

2.4.1. Establishment of the PSB consortium

To assess the compatibility of the best-performing PSB strains when assembled as a consortium the Kirby-Bauer test was applied (Irabor and Mmbaga, 2017). This methodology compares strains in pairs to detect potential inhibition areas between them. Briefly, after 24 h of incubation in liquid LB, strain 1 (PSB 1) was swabbed uniformly onto the LB plate surface using a sterile cotton swab and left to dry. Meanwhile, four sterile 5-mm Whatman discs (Cytiva, Milan, Italy) were aseptically dipped into a 24-hour-old suspension containing strain 2 (PSB 2) and placed at four equidistant points (approximately 1.5 cm from the edge of a 90-mm-diameter Petri plate) on the plate swabbed with PSB 1. The plates were incubated at 28 ± 2 °C and observed for potential inhibition areas over seven days. Each pairwise compatibility test was performed in triplicate.

2.4.2. Setting-up of the in vivo experimental system

The four best-performing PSB strains (*Pseudomonas graminis* PG0319 and PG1211; *Pseudomonas rhodesiae* PR0393; *Paraburkholderia terricola* PT0405) were selected based on their efficiency in solubilizing P under both pH conditions, cellulase activity and strain compatibility, and they were assembled to establish a PSB consortium for maize SC. SnHAs were selected to be used as the P source since they were more prone to bacterial solubilization than TnHAs. Maize (*Zea mays* cv. Lolita, Pioneer Hi-Breed, USA) was chosen as a model plant. Before SC, the germination rate was assessed according to the International Rules for Seed Testing (ISTA, 2023; https://www.seedtest.org/en/publications/international-ruleSseed-testing). Healthy and homogenous maize seeds (n = 150) were surface sterilized with NaClO and 70 % ethanol, washed with sterile dH_2O, dried and placed at 4 °C in the dark for 24 h before coating.

In detail, the PSB consortium was established by mixing an equal volume of each 22-hour-old PSB suspension to get the same bacterial abundance in the final inoculum (OD600nm = 0.5). The resulting PSB broth was mixed with an equal volume of sterile 2 % CMC to form a slurry in which maize seeds were dipped and stirred for 1 h. Once coated, seeds were dried under a laminar flow overnight. Control seeds were coated with CMC plus mock inoculum (double sterilized PSB broth). Before being transferred into the pots, the coated seeds were pre-germinated for seven days in the dark, and the germination rate was assessed (average of 95 %). Pre-germination was carried out in sterile Petri dishes (Ø 35 mm) containing a mixture of sterilized soil, vermiculite and quartz sand (1:1:1) (hereafter mixed substrate). Soil proprieties are reported in Table S2. The mixed substrate was autoclaved by two cycles (24 h apart) at 121 °C for 21 min and used for both pre-germination and pot experiments.

The SnHA (0.5 g) was applied to the substrate of each pot (10 × 10 × 14 cm^3: 1300 mL), placed at 7 cm from the bottom of the pot, and then covered with the mixed substrate. Pre-germinated seeds (one per pot) were transplanted 4 cm above and covered with the remaining mixed substrate. An additional PSB inoculum (PSB reinforcement) was also applied after transplanting to test a greater PSB density. Treatments were the following: (i) no SnHAs + mock-inoculum coated seeds (control: −S NB); (ii) no SnHAs + PSB seed coating (−S SC); (iii) no SnHAs + PSB seed coating + PSB reinforcement (−S BR); (iv) SnHAs + mock-inoculum coated seeds (+S NB); (v) SnHAs + PSB seed coating (+S SC); (vi) SnHAs + PSB seed coating + PSB reinforcement (+S BR). Pots were placed in a growth chamber at 25/18 °C day/night temperature, 16/8 h light/dark cycle, 65/50 % day/night humidity. The experiment was set up according to a completely randomized, and seven replicates for each treatment, for a total of 42 pots. Pots were watered every four days with deionized water, and every ten days with a modified Hoagland's solution (Hoagland and Arnon, 1950) having 1/4 of the quantity of P required achieving a minimum threshold for the plant (Gómez-Muñoz et al., 2018).

2.5. Samplings and analyses of maize growth and nutrient uptake

All samplings were performed after 34 days of growth, corresponding to stage 1 (GS1; Hanway, 1963), *i.e.*, maize plant with the collar of fifth leaf visible. Maize roots, stem, and leaves were sampled and, after oven-drying for 72 h, dry weight (DW) was recorded. Dry samples (approximately 0.3 g) of roots, stem and leaves were ground and mineralized in 8.0 mL of nitric acid (65 % trace grade, VWR, Milan, Italy) in Teflon vessels by microwaving (COOLPEX Smart Microwave Reaction System, Yiyao Instrument Technology Development Co., Ltd., Shanghai, China). Four replicates per treatment were analyzed. The solution was diluted with Milli-Q water to reach a final volume of 30 mL and filtered samples (Ø 0.45 mm) were analyzed for P and K by inductively coupled plasma-optical emission spectrometry (ICP-OES) using a spectrometer (Agilent Technologies, Italy).

The Phosphorus Use Efficiency (PUE) of SC and BR was calculated using the following formula:

$$PUE = \frac{\text{Maize P uptake with SnHAs}}{\text{P applied with SnHA}} \times 100$$

where:

Maize P uptake with SnHAs is the total P accumulation in maize plant fertilized with SnHAs, calculated as the sum of P concentration in each plant organ multiplied by its corresponding DW; P applied with SnHA corresponds to 18 % of the total of SnHA dose applied per pot, based on the concentration of P in SnHAs.

The Phosphorus Recovery Efficiency (PRE) of SC and BR was determined as:

$$PRE = \frac{(\text{Maize P uptake with SnHAs}) - (\text{Maize P uptake without SnHAs})}{\text{P applied with SnHAs}} \times 100$$

where:

Maize P uptake without SnHAs represents the P accumulation in the biomass of maize not fertilized with SnHAs, calculated as the sum of P concentration in each plant organ multiplied by its corresponding DW.

2.6. Primer design and real time RT-qPCR validation of plant P-related genes

At GS1, fresh roots were ground with liquid nitrogen for gene expression analysis (three replicates for each treatment). Total RNA was extracted from 100 mg of each sample using the RNeasy Mini Kit (Qiagen, Venlo, Netherlands). During the extraction, RNA was column-digested using the RNase-Free DNase Set (Qiagen, Venlo, Netherlands). Before reverse transcription to complementary DNA (cDNA), RNA extracts were checked for integrity, quantity, and purity by agarose gel electrophoresis (1 %), Qubit™ RNA HS Assay (Life Technologies, Thermo Fisher Scientific, Waltham, MA, USA), and Nanodrop (Thermo Fisher Scientific, Waltham, MA, USA). A total of 18 RNA extractions were performed (three replicates for each treatment). Each RNA extract (total RNA: 655 ng) was reverse transcribed to cDNA using the iScript™ Reverse Transcription Supermix (Biorad, California, USA). Specific primer pairs for P transporters were designed using the NCBI primer design tool (https://www.ncbi.nlm.nih.gov/tools/primer-blast/) (Table S3). Before real time RT-qPCRs, each primer pair was subjected to a thermal gradient amplification and primer efficiency. Only primer pairs having an efficiency between 90 % and 110 % were selected. Details on target P genes, primer names, sequences, and efficiency are reported in Table S3. The reaction mix for the real time RT-qPCR was performed in a total volume of 10 μL containing 1 μL of each cDNA (1:10), 5 μL of SsoAdvanced™ Universal SYBR® Green Supermix (Biorad, California, USA), 1 μL of each primer (10 μM), and 2 μL of nuclease-free water. The amplification cycle was as follows: an initial denaturation at 95 °C for 3 min, 39 cycles of denaturation at 95 °C for 10 s, and an annealing/extension at 59 °C for 30 s. The RTqPCR analyses were conducted in a CFX Connect Real-Time System (Biorad Laboratories, California, USA). After amplification, a melting curve analysis from 65 °C to 95 °C was generated to check primer specificity. Each 96-multi-well contained a control (nuclease free water; Qiagen, Venlo, Netherlands). For each sample three technical replicates were included. The analysis of the relative gene expression was performed according to the $2^{-\Delta\Delta C}_{T}$ method (Livak and Schmittgen, 2001). The transcript level of the plant genes in −S NB was used as control, and the polyubiquitin containing 7 ubiquitin monomers as reference gene (Pii et al., 2016).

2.7. Quantification of the bacterial biomass in the substrate and maize roots

The bacterial biomass in the substrate and maize roots was measured as a proxy of persistence of PSB inoculum. DNA was extracted from the substrate and maize roots (four replicates for each treatment for a total of 24 samples for substrate and 24 samples for roots) using the DNeasy PowerSoil Kit (Qiagen, Venlo, Netherlands), following the manufacturer's instructions. Bacterial biomass was analyzed by a quantitative PCR (qPCR) (Fierer et al., 2005) approach using the Eub338/Eub518 primer pairs (Eub338: 5′-ACTCCTACGGGAGGCAGCAG-3′; Eub518: 5′-ATTACCGCGGCTGCTGG-3′), targeting the 16S rRNA gene (Vilgalys and Hester, 1990; Lane, 1991; Gardes and Bruns, 1993; Muyzer et al., 1993). The analyses were conducted in a CFX Connect Real-Time System (Biorad Laboratories, California, USA) with the following thermal program: an initial denaturation at 95 °C for 15 min, followed by 40 cycles of 95 °C for 1 min, 53 °C for 30 s, and 72 °C for 1 min, followed by a melting curve analysis from 58 °C to 65 °C. The qPCR reactions mix was as described above. Each 96-well plate also contained reactions with two-fold serial dilutions of pure bacterial DNA (*Streptomyces rochei* DSM 41732) to verify the linearity of the relationship between threshold cycle (Ct) and DNA concentration. Standard curves were generated using a triplicate of plasmids. Each sample was run in triplicate, and the mean Ct value was used for the calculation of the 16S rRNA gene copies. Results refer to one gram of substrate or root dry weight.

2.8. Statistical analysis

One-way ANOVAs were performed to analyze the effect of PSB strain (fixed factor) on PSI measured on β-TCP plates, IAA and cellulase production. For PSI, each pH condition was analyzed separately. Two-way ANOVAs were conducted to test the effect of the PSB strain and time point (fixed factors), and their interaction on solubilization efficiency and solubilized P in β-TCP, SnHAs and TnHAs liquid media for each pH condition separately. Similarly, a two-way ANOVA was used to test the effect of the application of PSB (NB, SC, and BR), SnHAs (−S; +S), and their interaction on maize growth and nutrient uptake. Following ANOVAs, *post hoc* Tukey-B test was performed for testing significant differences ($P \leq 0.05$) among samples. Percentage data were transformed prior statistical analyses. One-way ANOVA was used to analyze PUE and PRE using +S NB, +S SC, and +S BR as treatments. Moreover, linear regressions were generated to model the relationship between pH (independent factor) in β-TCP, SnHAs and TnHAs media, and solubilized P (dependent factor) over time for each pH condition.

A *t*-test was conducted to compare the relative expression of P-related genes in the roots of maize treated with SnHAs (−S; +S) across different PSB treatments (NB; SC; BR). Each test compared the $2^{-\Delta\Delta C}_{T}$ of a specific treatment against a reference group, *i.e.*, −S NB. Similarly, a t-test was employed to compare the bacterial abundance in soil and maize roots under each treatment against S NB. All univariate analyses were conducted using the SPSS 25.0 software package (SPSS Inc., Chicago, IL, USA), and results were plotted using *ggplot2* package (Wickham and Wickham, 2016) in R.

A permutational multivariate analysis of variance (PERMANOVA) was applied to investigate the effect PSB strain (fixed factors) and substrate (β-TCP, SnHAs, and TnHAs) on the OA profile at each pH (three replicates for each treatment). Data were normalized and the Euclidean distance matrix was calculated. *P* values were calculated using 999 permutations, together with the explained variance by factors. The dispersion among samples was tested by the analysis of multivariate homogeneity (PERMDISP). PERMANOVA pairwise comparisons were performed for PSB strain and substrate. PERMANOVA was also performed, as described above, to test the effect of PSB treatment (NB, SC, BR), SnHAs (−S, +S), and its interaction on maize growth, P and K plant uptake, and P-related gene expression in roots (three replicates for each treatment). The PERMDISP was also conducted. Then, the principal coordinate analysis (PCoA) was performed to visualize the relevant patterns.

To understand the relationship between the efficiency in solubilizing P (*i.e.*, % of solubilized P in the *in vitro* system at T3, T5 and T7) and OA production of the strains included in the PSB consortium (independent variables) and plant parameters (*i.e.*, plant growth, P uptake and gene expression; dependent variables), and to identify the main traits responsible for plant functional changes, a multivariate statistical approach (RELATE analysis) was applied. The RELATE analysis allows to determine the strength of the correlation between two matrices in rank-order patterns of dissimilarity (Clarke and Warwick, 2001). The treatments +S NB and +S SC of the *in vivo* systems, and the same treatments in the *in vitro* system conducted at pH 7.5, were utilized for the analysis. We utilized the matrix of data collected in the *in vitro* system at pH 7.5 since the value was similar to the pH of the soil utilized in the *in vivo* experiment. The data matrices of the independent and dependent variables were normalized, and Euclidean distance resemblances were calculated. The analysis was based on the Spearman rank and 999 permutations with ρ equal to 1 representing the perfect relationship,. Since the RELATE was significant, we displayed the paraments of both matrices using PCoA biplots. To find the best descriptor of the relationship, the BEST analysis, based on BioEnv methods (all

combinations), Spearman rank, and 999 permutations, was applied (Clarke et al., 2008). PERMANOVAs and PERMDISP were performed using the *vegan* R package (Oksanen et al., 2020). Pairwise comparisons were performed using the *pairwiseAdonis* R package (Martinez Arbizu, 2020). PCoA biplots were generated by the *stats* package. RELATE and BEST analyses were performed using PRIMER 7 and PERMANOVA + software (Clarke and Gorley, 2015; Anderson et al., 2008).

3. Results

3.1. Phosphate solubilization activity by PSB

In the qualitative *in vitro* screening, none of the 15 strains, including the strong solubilizers (*e.g.*, *P. graminis* PG0319), showed solubilization activity, *i.e.* a solubilization halo around the colony, when inoculated on SnHAs, TnHAs, MnHAs, $AlPO_4^-$ and $FePO_4^-$ (Fig. S3). In β-TCP, the PSB strains exhibited a solubilization activity ranging from weak to strong, under both acidic and alkaline conditions (Table S4). Examples of weak, mild and strong solubilization activities are illustrated in Fig. 1a. Details about the results of the qualitative screening are given in Supplementary Results 1.

In the quantitative *in vitro* screening, the percentage of solubilized P in all substrates and pH conditions was affected by the interaction between PSB strain and time (Table S5). In β-TCP, under acidic pH conditions, the average over time of the percentage of solubilized P of the PSB strains was 54 % (Fig. 2). Over time, PG0319 achieved 77 % solubilization of P, followed by PR0393, PG1211, PC1218 and PT0405 with 75 %, 68 %, 50 % and 49 %, respectively. PP0616 exhibited the lowest average value of 15 %. Most strains demonstrated a time-dependent increase in the solubilization efficiency, with a consistent 10 % rise from T3 to T7. For example, PG0319 solubilized 68 % at T3, 75 % at T5, and 83 % at T7. PG1211, PC1218, PR0393 and PF0504 also exhibited this upward trend, whereas PT0405 and PP0616 reached their highest solubilization at T3 and T5, respectively, before declining at T7. Under alkaline pH, the average over time of the percentage of solubilized P was 48 %, with PG0319 similarly showing the highest value (77 %) and PP0616 the lowest (10 %). Consistently under acidic conditions, the best-performing strains were PG0319, PG1211, PC1218 and PR0393, which maintained a high efficiency over time, with the highest solubilization observed at T5. In addition, PT0405 and PP0616 substantially

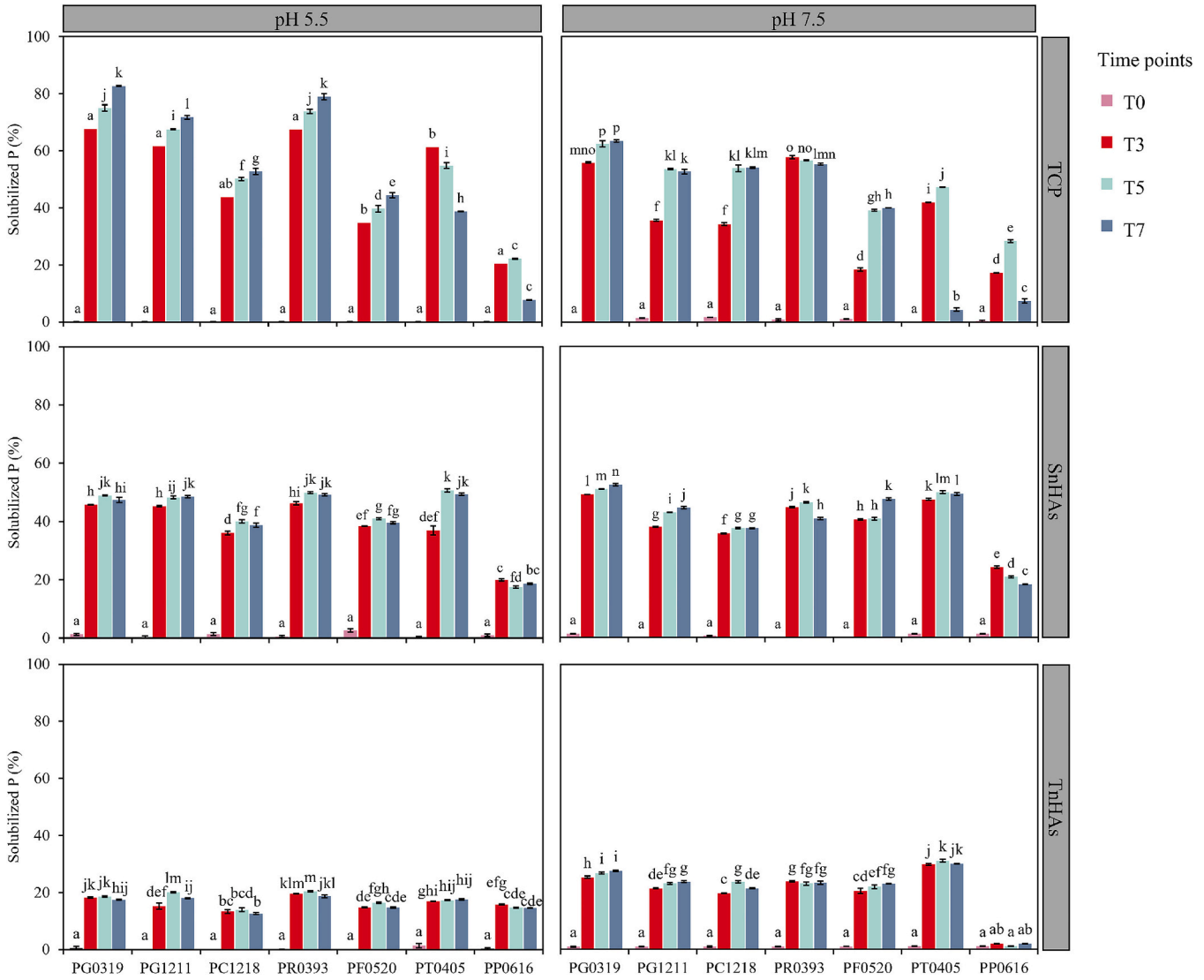

Fig. 2. Solubilized phosphorus (P) (%) in liquid media across four time points (T0, T3, T5, and T7) by selected phosphate-solubilizing bacteria (PSB) in tricalcium phosphate (TCP), salmon hydroxyapatite nanoparticles (SnHAs) and tuna hydroxyapatite nanoparticles (TnHAs) under acidic and alkaline pH (5.5 and 7.5, respectively). See Table 1 for PSB identities. Data are mean ± SE (n = 4). Different letters represent significant differences among PSB strains and time points, according to two-ways ANOVA and *post hoc* Tukey-B test ($P \leq 0.05$) (see Table S4 for *P* values).

decreased their activity at T7 after their peak at T5.

In SnHAs, PSB strains showed a lower percentage of solubilized P over time. Averaged over PSB strains, the solubilization efficiency was 42 % under both acidic and alkaline conditions (Fig. 2). At pH 5.5, PR0393 achieved the highest rate (54 %), followed by PG0319, PG1211 and PT0405 (52 %). In contrast, strains PC1218 and PF0520 demonstrated intermediate efficiencies (37 % and 39 %, respectively), whereas PP0616 had the lowest rate (10 %). The maximum efficiency was observed at T5, with an average of 55 % among the top strains (PG0319, PG1211, PR0393 and PT0405). At pH 7.5, the solubilization efficiency of the best-performing strains remained stable. Notably, efficiency increased progressively over time, reaching the peak at T7, with the top strains reaching on average 50 %.

In TnHAs, the overtime average percentage of solubilized P was lower compared to β-TCP and SnHAs under both pH conditions (Fig. 2). Despite this, significant differences were observed among strains. At acidic pH, the best performers were PR0393, PG0319, PG1211 and PT0405, with an average of efficiency of 12 %, 10 %, 10 % and 9 %, respectively, and a peak at T5. At alkaline pH, all strains performed better, with a general maximum solubilization at T7. For instance, strains PT0405 and PG0319 showed increases of 65 % and 50 % in efficiency, respectively, compared to acidic pH. The pattern of changes of the amount of solubilized P (mg L^{-1}) across substrates and pH conditions, was similar to the pattern observed when calculated using the total P content in β-TCP, SnHAs and TnHAs (Fig. S4).

Most PSB strains significantly lowered the pH in all substrates at both pH conditions, whereas ineffective strains, like PP0616, did not affect pH in the liquid medium (Fig. S4). Under acidic pH, a negative moderate relationship between the pH and the amount of solubilized P was observed ($R = 0.511$; $P < 0.001$) (Fig. S4a), while a stronger relationship was found under alkaline pH ($R = 0.690$; $P < 0.001$) (Fig. S4b).

3.2. Organic acids secreted by PSB

Under both pH conditions, PERMANOVA indicated that the interaction between PSB strains and substrate was significant ($P < 0.001$) (Table S6). The PSB strains secreted different OAs across substrates (*i.e.*, TPC, SnHAs, and TnHAs). The variance explained by the interaction was 30 % and 38 % at pH 5.5 and 7.5, respectively. The patterns are visualized in the PCoA biplots in Fig. 3, and PERMANOVA pairwise comparisons of the interaction PSB strain and substrate are shown in Table S7. As an example, under acidic and alkaline conditions, PG0319 inoculated in TCP produced gluconic acid, while in SnHAs it produced fumaric acid (Fig. 3). The same strain inoculated in TnHAs secreted fumaric acid at a lower concentration under acidic conditions (Fig. 3a), and acetic acid and propionic under alkaline conditions (Fig. 3b).

3.3. Maize growth, nutrient uptake, and P-use efficiency

The selected best-performing PSB strains used as consortium for maize seed coating (*i.e.*, *P. graminis* PG0319 and PG1211, *P. rhodesiae* PR0393, and *P. terricola* PT0405) were compatible since they did not

Table 2
Effect of the interaction between inoculation with phosphate-solubilizing bacteria (PSB) and application of salmon hydroxyapatite nanoparticles (S) on roots, stem, leaves and total plant dry weight (DW; g $plant^{-1}$) of *Zea mays* (L.) at growth stage 1 (GS1).

	DW			
	Roots	Stem	Leaves	Total plant*
−S†				
NB‡	0.91 ± 0.06 ab§	0.71 ± 0.03 a	0.47 ± 0.02 ab	2.10 ± 0.08 a
SC	1.09 ± 0.03 c	0.91 ± 0.03 cd	0.57 ± 0.03 bc	2.57 ± 0.09 b
BR	1.12 ± 0.03 c	1.03 ± 0.03 d	0.60 ± 0.03 c	2.75 ± 0.10 b
+S				
NB	0.80 ± 0.03 a	0.75 ± 0.03 b	0.47 ± 0.02 ab	2.02 ± 0.05 a
SC	1.03 ± 0.05 bc	0.90 ± 0.03 bcd	0.53 ± 0.02 abc	2.46 ± 0.09 b
BR	0.85 ± 0.03 a	0.77 ± 0.03 abc	0.43 ± 0.02 a	2.05 ± 0.08 a
P (PSB)	**<0.001**¶	**<0.001**	**0.049**	**<0.001**
P (S)	**<0.001**	0.085	**0.006**	**0.006**
P (PSBxS)	**0.025**	**<0.001**	**0.004**	**<0.001**

* Total plant is the sum of roots, stem, and leaves.
† −S = no application of SnHAs; +S = application of SnHAs.
‡ NB = mock inoculum coated seeds; SC = PSB seed coating; BR = PSB seed coating + PSB reinforcement.
§ Values are mean ± SE. Values within the same column followed by different letters indicate significant differences according to a two-way ANOVA and the *post hoc* Tukey-B test ($P \leq 0.05$) (seven replicates).
¶ In bold significant *P* values.

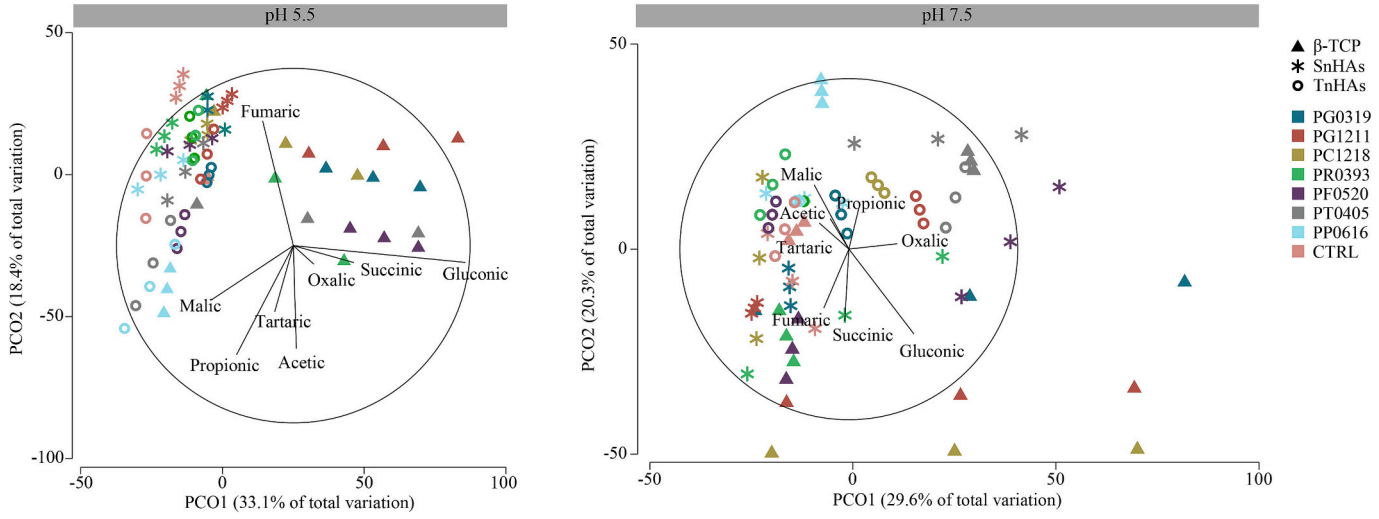

Fig. 3. Principal coordinate analysis (PCoA) biplot based on the significant effects of PSB strains, substrates, and their interaction on the organic acid (OA) production at acidic (pH 5.5) and alkaline conditions (pH 7.5). Data were normalized and the Euclidian distance matrix of similarity calculated. See Table S5 for PERMANOVA for significant values.

Table 3
Effect of the interaction between inoculation with phosphate-solubilizing bacteria (PSB) and application of salmon hydroxyapatite nanoparticles (S) on phosphorus (P) and potassium (K) content (mg plant^{-1}) in roots, stem, leaves, and total plant of *Zea mays* (L.) at growth stage 1 (GS1).

	P				K			
	Roots	Stem	Leaves	Total plant *	Roots	Stem	Leaves +	Total plant
−S†								
NB‡	1.16 ± 0.19 ab §	1.34 ± 0.27 a	0.96 ± 0.09 a	3.46 ± 0.39 a	36.07 ± 4.08 abc	76.03 ± 6.71 a	37.44 ± 2.61 a	149.54 ± 10.41 a
SC	1.29 ± 0.20 bc	1.83 ± 0.24 bc	1.31 ± 0.10 bc	4.43 ± 0.43 bc	31.83 ± 1.16 ab	97.90 ± 2.63 b	51.49 ± 1.47 bc	181.23 ± 4.11 bc
BR	1.16 ± 0.08 ab	2.03 ± 0.08 c	1.46 ± 0.05 c	4.65 ± 0.14 c	41.45 ± 2.42 bc	102.93 ± 0.93 b	59.01 ± 4.60 a	203.38 ± 4.91 c
+S								
NB	0.95 ± 0.07 a	1.54 ± 0.05 ab	1.19 ± 0.22 abc	3.68 ± 0.25 a	24.31 ± 0.85 a	88.09 ± 1.25 ab	38.97 ± 1.45 a	151.37 ± 2.40 a
SC	1.56 ± 0.19 c	1.90 ± 0.14 bc	1.24 ± 0.09 bc	4.70 ± 0.34 c	44.43 ± 3.95 c	97.12 ± 2.04 b	45.78 ± 0.83 ab	187.33 ± 5.90 bc
BR	0.98 ± 0.05 ab	1.73 ± 0.13 bc	1.14 ± 0.11 ab	3.84 ± 0.27 ab	29.12 ± 1.59 a	89.89 ± 4.22 ab	42.86 ± 1.96 ab	161.88 ± 7.42 ab
P (PSB)	**<0.001**¶	**<0.001**	**0.025**	**<0.001**	0.170	**0.003**	**0.004**	**0.001**
P (S)	**0.005**	**0.029**	**0.001**	**0.006**	0.280	0.899	0.056	0.244
P (PSBxS)	**0.005**	**0.029**	**0.001**	**0.006**	**<0.001**	**0.010**	**0.007**	**0.003**

* Total plant is the sum of roots, stem, and leaves.
† −S = no application of SnHAs; +S = application of SnHAs.
‡ NB = mock inoculum coated seeds; SC = PSB seed coating; BR = PSB seed coating + PSB reinforcement.
§ Values are mean ± SE. Values within the same column followed by different letters indicate significant differences according to a two-way ANOVA and the *post hoc* Tukey-B test ($P \leq 0.05$) (four replicates).
¶ In bold significant *P* values.

produce any inhibition halo and were able to grow simultaneously on plates (data not shown). Significant interactions between PSB inoculation (NB, SC, BR) and SnHAs (−S, +S) application were observed for all maize growth parameters and nutrient uptakes (Table 2; Table 3). With no SnHAs, the application of PSB strains either as SC or BR significantly promoted root and total plant DW compared to the control (NB) (+11 % and 27 %, respectively) (Table 2). Consistently, stems and leaves significantly increased. By contrast, with SnHAs only SC increased root and total DW compared to NB (+29 % and 22 %), reaching values similar to −S SC and −S BR. Stem and leaf DW did not differ among treatments with SnHAs.

In roots, P content significantly improved with +S SC, showing a 47 % increase compared to other treatments, except for −S SC exhibiting similar values (Table 3). Stem, leaf, and total P content was enhanced by PSB without SnHAs (+40 % on average). Similarly, when SnHAs was applied, SC and BR enhanced P in stems and leaves compared to −S -NB (+36 % and 24 %, respectively), although no variation was reported with respect to +S NB. Notably, +S SC increased total plant P content compared to −S and +S NB (+32 %), reaching values similar to PSB without SnHAs.

With the application of SnHAs, PUE and PRE, used as indexes of sustainability of P application and potential environmental risks, were significantly enhanced by seed coating (+S SC), increasing by 25 % and three-fold, respectively, compared to the application of SnHAs alone or with bacterial reinforcement (+S BR) (Fig. 4a,b). Treatments +S NB and +S BR showed similar P-use efficiencies.

Seed coating with SnHAs promoted root K content compared with other treatments (+66 %), whereas without SnHAs no difference was

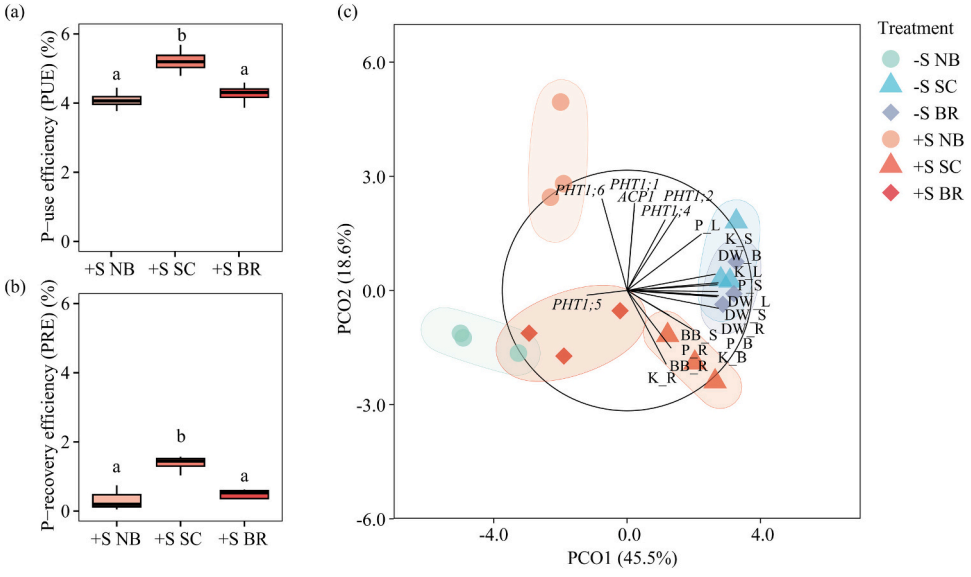

Fig. 4. P-use efficiency (a) and P-use recovery (b) of the application of salmon hydroxyapatite nanoparticles (SnHAs; +S) and PSB inoculation (no bacteria, NB; seed coating, SC; bacterial reinforcement, BR). Boxplots show median, first and third quartiles, and minimum and maximum values. Four replicates per each treatment. Different letters represent significant differences among treatments, according to one-way ANOVA and *post hoc* Tukey-B test ($P \leq 0.05$). Principal coordinate analysis (PCoA) biplot (c) on the effects of the application of PSB (NB, SC, BR) and SnHAs (no SnHAs, −S; SnHAs, +S) on: dry weights (DW) and nutrients (P, K) in roots (R), stem (S), leaves (L), total biomass (B); relative expression of P-related genes (*PHT1;1, PHT1;2, PHT1;4, PHT1;5, PHT1;6, ACP1*) in roots, and total bacterial biomass (BB) in the substrate (S) and in roots (R). The output is based on the significant effect of the interaction between the two factors following PERMANOVA (see Table S8).

observed among treatments (Table 3). Stem and leaf K content did not change after applying PSB and SnHAs in comparison to +S NB, but it increased under +S SC compared to −S NB (+32 %). Similarly, without SnHAs, BR promoted K stem content (35 %) compared to −S NB, and reached the highest total plant K uptake among all treatments. Moreover, −S SC and +S SC promoted total K content with respect to NB with and without SnHAs (+22 %).

3.4. Expression of P-related genes in roots of maize and quantification of bacterial biomass

Several genes, such as *PHT1;1, PHT1;2, PHT1;4 and PHT1;6*, displayed significant upregulation under specific treatments compared to −S NB, while *PHT1;5* and *ACP1* remained unaffected (Fig. 5). The expression of *PHT1;1* significantly increased by 113 % and 53 % under +S NB and +S SC treatments, respectively. Moreover, *PHT1;2* significantly increased by 50 % under −S BR, and by 27 %, 30 % and 67 % under BR, SC and NB with SnHAs. The relative expression of *PHT1;4* significantly increased under SC and BR without SnHAs (53 % and 73 %, respectively), as well as by applying +S NB (50 %). *PHT1;6* was significantly upregulated by −S BR, and by +S BR and +S NB (80 %, 120 % and 320 %, respectively). Bacterial biomass in the substrate, measured as 16S gene copies per g of soil, significantly increased in −S SC (+20 %) compared to −S NB, while no effects were observed in other treatments (Fig. 6a). In the roots, −S BR and +S BR significantly increased bacterial biomass by +12 % and 11 %, respectively, compared to −S NB (Fig. 6b).

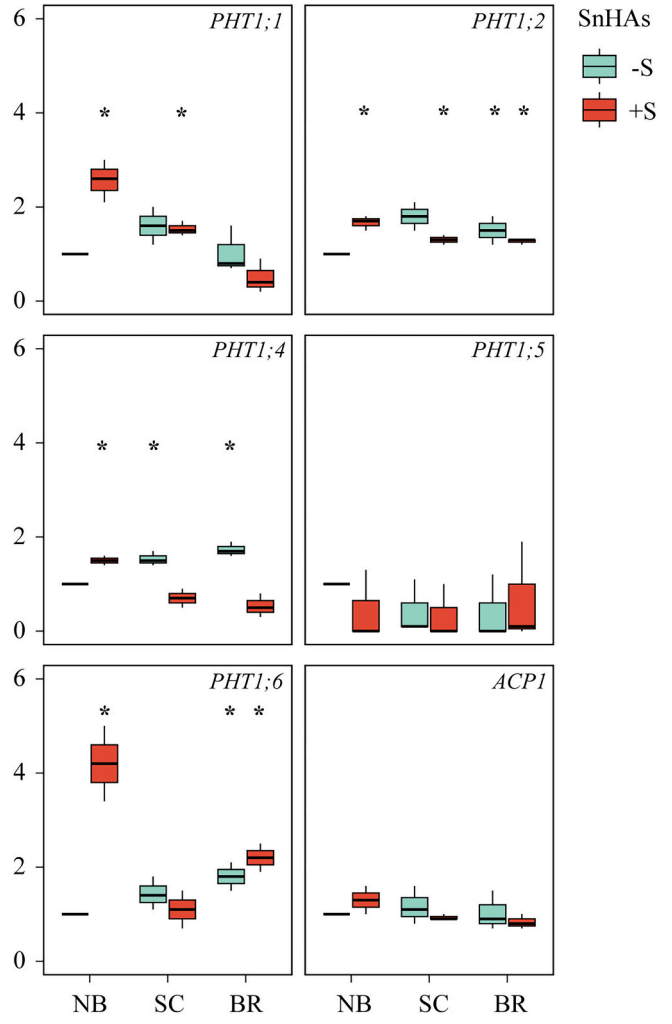

Fig. 5. Relative expression of P-cycle related genes, such as P transporters (*PHT1;1, PHT1;2, PHT1;4, PHT1;5, PHT1;6*) and acid phosphatase 1 (*ACP1*), in maize roots after phosphate-solubilizing bacteria (PSB) inoculation (seed coating, SC; seed coating + PSB reinforce, BR) and salmon hydroxyapatite nanoparticles (SnHAs) application (no SnHAs, −S; SnHAs, +S). The relative expression of genes was determined by double standardisation method (Livak and Schmittgen, 2001) using the transcript level of the reference gene polyubiquitin containing 7 ubiquitin monomers (poliub7) and that of the control (no SnHAs, no bacteria; −S NB). Boxplots show median, first and third quartiles, and minimum and maximum values. Three replicates per each treatment, and three technical replicates for each sample. Different symbols represent significant differences between the control and treatments according to *t*-test (* $P \leq 0.05$; ** $P \leq 0.001$; *** $P \leq 0.0001$).

3.5. Overall effect of PSB and SnHAs on plant and soil parameters

PERMANOVA revealed a significant interaction between PSB inoculation and SnHAs application on plant and soil parameters ($P < 0.001$), which explained 50 % of the total variation (Table S8). The PCoA biplot confirmed the complex interactions between these two factors (Fig. 4c). The treatments −S SC and −S BR clustered together, and had a pattern similar to +S SC, promoting plant growth and nutrient parameters in above-ground tissues. Additionally, +S SC strongly increased bacterial biomass in substrate and roots, along with P and K content in roots. Treatments −S NB, +S NB and +S BR showed similar patterns among each other, showing a high relationship with the expression of *PHT1;5*. By contrast, +S NB was related to a greater expression of *PHT1;1*, *ACP1* and *PHT1;6* genes. Overall, *PHT1;2* and *PHT1;4* genes were highly correlated, as well as *PHT1;1*, *ACP1* and *PHT1;6,* whereas *PHT1;5* clustered alone.

3.6. Mechanisms of plant P uptake

The functional response of maize was highly related to the solubilization efficiency of the PSB strains and to the secreted OAs at T7 in the *in vitro* system, as supported by the significance of RELATE analysis ($\rho = 0.706$; $P = 0.016$). This relationship is clear when comparing the bacterial parameter patterns in the *in vitro* system and the plant patterns displayed in the PCoA plots (Fig. S7a,b). Moreover, the BEST analysis highlighted the best predictors of plant functionality ($\rho = 0.861$, $P = 0.014$), namely propionic acid considering one descriptor ($r = 0.780$), or the solubilization efficiency at T7 and propionic acid considering two descriptors ($r = 0.834$) (Fig. 7c). These BEST predictors were also

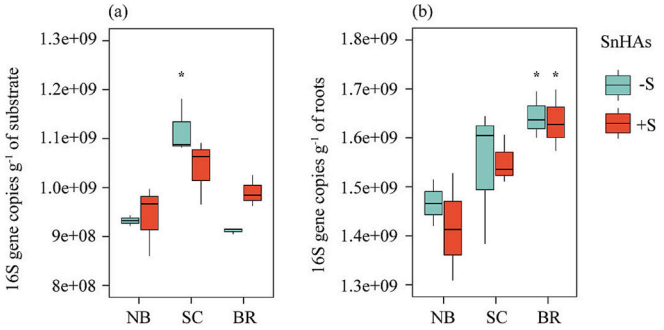

Fig. 6. Bacterial biomass in the substrate (a) and maize roots (b) after phosphate-solubilizing bacteria (PSB) inoculation (seed coating, SC; seed coating + PSB reinforce, BR) and salmon hydroxyapatite nanoparticles (SnHAs) application (no SnHAs, −S; SnHAs, +S). The 16S rRNA gene copy number was determined according to Fierer et al. (2005), using standard curves generated by two-fold dilutions of pure bacterial DNA (*Streptomyces rochei* DSM 41732). Ct value was used to calculate 16S gene copies. Results were referred to one gram of roots and substrate. Boxplots show median, first and third quartiles, and minimum and maximum values. Three replicates per each treatment, and three technical replicates for each sample. Different symbols represent significant differences between the control and treatments according to t-test (* $P \leq 0.05$; ** $P \leq 0.001$; *** $P \leq 0.0001$).

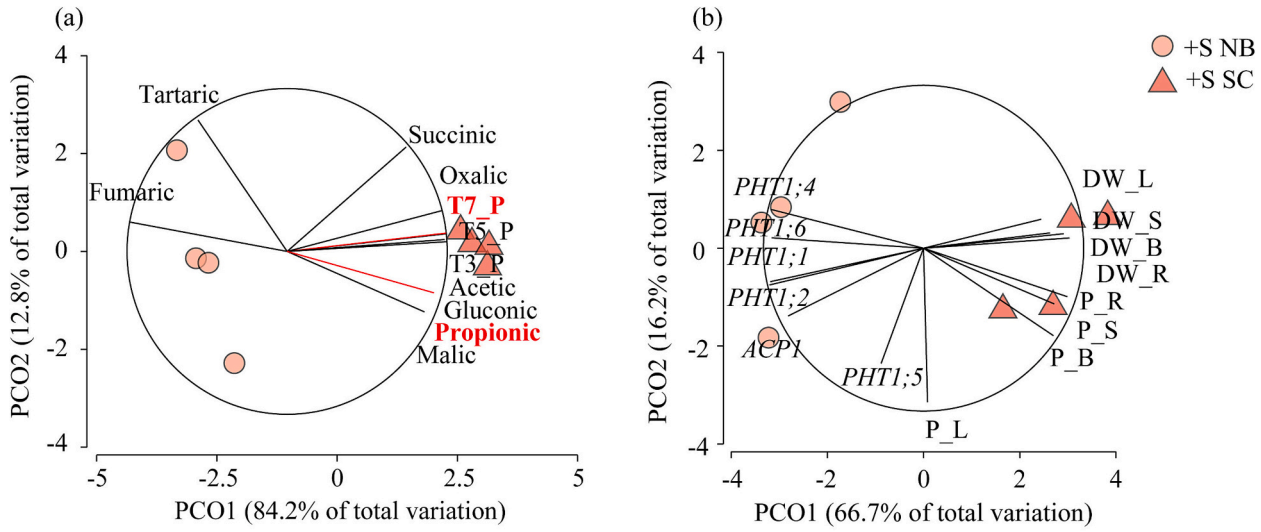

(c)

BEST results

Global test	ρ	*P*
	0.861	0.014
No.Vars	Corr.	Selections
1	0.780	Propionic
2	0.834	**T7, Propionic**
3	0.850	Fumaric, Succinic, Propionic
4	0.861	T7, Fumaric, Succinic, Propionic
5	0.858	T3, T7, Fumaric, Succinic, Propionic

Fig. 7. Principal coordinate analysis (PCoA) biplot (a) of the efficiency in solubilizing P (*i.e.*, % of solubilized P at T3, T5 and T7) and organic acid (OA) production in the *in vitro* system of the PSB strains included in the consortium together with the salmon hydroxyapatite nanoparticles (SnHAs) (+S SC), and of the salmon hydroxyapatite nanoparticles applied alone (+S NB) under alkaline pH. PCoA biplot (b) of the plant traits (*i.e.*, plant growth, P uptake and gene expression) measured in the *in vivo* system for the treatments +S NB and +S SC. In the PCO plot the vectors in red are those significant based on the BEST analysis. Results of the BEST analysis (c) based on BioEnv methods (all combinations), Spearman rank, and 999 permutations for identifying the best descriptor of the significant relationship between the two matrices: PSB traits in the *in vitro* system (independent variables) and plant parameters in the *in vivo* system.

highlighted in red the PCoA plot (Fig. S7a).

4. Discussion

4.1. In vitro mechanisms of P solubilization

The characterization of the two forms of nHAs derived from different by-products revealed clear differences: SnHAs contained both β-TCP and HA, while TnHAs were pure HA (Fig. S1a), which is known to be less soluble (Dorozhkin and Epple, 2002). FTIR analysis confirmed β-TCP in SnHAs, along with CO_3^{2-} and -OH groups (Fig. S1b), which may enhance solubility and stability in aqueous environments (Dorozhkin, 2010; Pan and Darvell, 2010). Surface charge analysis showed SnHAs had a more negative charge than TnHAs (Fig. S1c), a factor influencing P availability, as negatively charged nHAs increase P diffusion in acidic soils (Xiong et al., 2018b). The ζ also indicated that SnHAs were more stable in solution. Additionally, SEM micrographs showed SnHAs as spherical particles (<50 nm) and TnHAs as rod- or needle-shaped grains (300 nm) (Fig. S1d–g), impacting dissolution rates and mobility due to differences in surface area (Sasson et al., 2007). All parameters indicated that SnHAs may offer greater P availability compared to TnHAs. When nHAs were tested in the qualitative *in vitro* screening, the 15 PSB strains showed a feeble solubilization of SnHAs, and no solubilization of TnHAs (Fig. S3) likely due to their weak solubility, as reported by Dorozhkin (2010) studying the solubility of HA-derived compounds. However, it is important to note that, consistent with our findings, other researchers have reported that plate assays can be misleading for weakly soluble P forms (Bashan et al., 2013a; Santana et al., 2019). Indeed the experiments performed in liquid confirming the ability of PBS of solubilizing also HA and not just β-TCP. Concerning TnHA, in fact, some solubilization in liquid took place, although to a smaller extent than in SnHA. Considering that TnHA is constituted almost exclusively by HA (see Fig. S1a and S1b), the solubilized P has to come from HA and not from β-TCP.

Among the six tested P substrates, β-TCP proved to be the most suitable substrate for preliminary discrimination of PSB strains (Fig. S3). On β-TCP, outstanding strains under both pH conditions comprised *Pseudomonas* species (*P. graminis, P. rhodesiae, P. corrugata*) (Table S4), which are widely considered strong P solubilizers (Rodriguez and Fraga, 1999; Alori et al., 2017). Similarly, *Paraburkholderia* species (*P. terricola, P. phytofirmans*), recently gained attention as promising novel P solubilizers (Hsu et al., 2018; do Amaral Leite et al., 2024), also outperformed.

To ensure a more reliable assessment of PSB effectiveness for agricultural applications, it is crucial to avoid relying solely on β-TCP as selection factor. Integrating quantitative assays offers a more realistic measure of PSB performance, especially when aiming at using less soluble P compounds such as nHAs (Bashan et al., 2013a,b). Indeed, in our study, quantitative screenings demonstrated the potential of SnHAs as a viable P substrate, as they were more readily solubilized by PSB compared to TnHAs (43 % *vs* 16 %) (Fig. 2; Fig. S4). The assessment conducted at different time points and varying pH conditions was also

pivotal for elucidating the kinetics and mechanisms of nHAs solubilization. In fact, we found that nHAs solubilization kinetics followed a species- and time-dependent pattern. For instance, some *Pseudomonas* species (*e.g.*, *P. graminis*, strains PG0319 and PG1211) exhibited a time-dependent increase in nHA solubilization, whereas *P. rhodesiae* and *P. terricola* showed a decline in activity by day five (Fig. 2). Oscillatory kinetics during P solubilization of nHAs were also reported by Delvasto et al. (2006), observing an initial rapid phase, followed by a rise-and-fall pattern. They attributed this pattern to re-precipitation processes, particularly to the formation of brushite ($CaHPO_4{\cdot}2H_2O$), which re-dissolves and contributes to the fluctuation of P concentrations. The solubilization dynamics were linked to pH stabilization and mineralogical changes, as suggested by Illmer and Schinner (1995), indicating complex interactions among microbial activity, pH changes, and P re-precipitation.

In addition, our study emphasized that a decrease in pH correlates with a greater P solubilization, under both pH conditions, although under acidic conditions the correlation was stronger (Fig. S5). The acidification of the surrounding environment is considered as one of the main consequences of the solubilization of Ca-P minerals by PSB (Raymond et al., 2021). Thus, acidic environments could have enhanced P solubility from nHAs. This was also reported by Xiong et al. (2018b) who investigated P availability of nHAs in an Ultisol and a Vertisol, characterized by acidic and alkaline pH, respectively. They found that in Ultisol, nHAs increased P availability due to their high dissolution under acidic conditions. This trend was also highlighted by Dorozhkin (2012), who found that the dissolution rates of HA increase with decreasing pH, which is a common observation in mineral dissolution. The process was explained by surface protonation, which weakens Ca—O bonds, thus accelerating dissolution.

However, certain factors can influence HA and nHAs solubilization even in alkaline environments, such as the biosynthesis of OAs by PSB which can facilitate the release of phosphate ions (Wang et al., 2016; Alori et al., 2017; Monroy Miguel et al., 2020). In the present work, the analysis of OA production in SnHAs and TnHAs highlighted strain- and substrate-specific metabolic profiles of the seven selected PSB at both pH (Fig. 3). For instance, the production of gluconic acid was particularly high when the four best-performing PSB strains were inoculated with β-TCP (*P. graminis*, PG0319 and PG1211; *P. rhodesiae*, PR0393; *P. terricola*, PT0405). Accordingly, the ability of gluconic acid to bind Ca^+ ions and enhance P solubilization is widely reported for mineral P forms (Farhat et al., 2015), especially for Gram-negative bacteria such as our inoculants. Indeed, Gram-negative bacteria were reported to oxidase glucose to gluconic acid (Sharma et al., 2015). The fact that PG0319 and PG1211 shifted the metabolism to produce acetic acid under alkaline conditions when applied with HAs, especially with SnHAs (Fig. S6) is noteworthy. Conversely, PT0405 produced acetic acid in solubilizing SnHAs and TnHAs under acidic pH. This pH-dependent metabolism underlines the adaptation of the strains in solubilizing P across different P sources and environmental conditions. Strain PR0393 demonstrated a more substrate-specific solubilization ability, particularly excelling in solubilizing TnHAs, suggesting specialized mechanisms, based on the secretion of fumaric acid, for the solubilization of P for that substrate. The strain PT0405 stood out for its broad metabolic flexibility. In fact, it produced a wider range of OAs, including gluconic, acetic and propionic acids, contributing to its effectiveness in solubilizing both SnHAs and TnHAs. Its OA production under both acidic and alkaline pH conditions indicates the suitability of strain PT0405 to be used in diverse environments in which variable soil pH affects P availability. To the best of our knowledge, only a few studies focused on the effects of OAs in the nHA dissolution mechanism (Wang et al., 2016; Priyam et al., 2019; Monroy Miguel et al., 2020). Our findings on OA production with nHAs are consistent with the results of Priyam et al. (2019), who reported that gluconic acid, among all studied OAs, showed the most significant correlation with nHA solubilization by *Bacillus licheniformis*. Accordingly, some *Pseudomonas* strains were previously reported to secrete gluconic acid to solubilize bulk rock phosphate (Hameeda et al., 2006). However, contrasting results were found by Monroy Miguel et al. (2020), who reported that none of the studied PSB species produced gluconic acid while solubilizing nHAs. They found that the nHA dissolution rate was higher when citric acid was applied, followed by oxalic and then acetic acid. Although acetic acid was found to be the least effective in solubilizing P in the short-term, it might be the most successful in providing P to crops in the long-term.

The four best-performing PSB strains demonstrated IAA production and N_2 fixation, except for PT0405 which demonstrated an appreciable IAA production, but no N_2 fixation ability (Fig. 1b-e). Multi-strain and multi-species consortia can provide complementary plant-beneficial functions, resulting in stronger cumulative benefits over single-specie inocula (Hassani et al., 2018; Liu et al., 2023). For example, consortia including isolates both producing IAA, solubilizing inorganic P, and fixing N_2 proved more effective for enhancing plant growth than individual strains (Kumar et al., 2016; Shilev et al., 2020). When designing bacterial consortia using different strains and species, a key aspect is to verify the interactions among them in terms of compatibility (Minchev et al., 2021). Therefore, in our study, we observed no antagonistic activity among strains, and thus we proceeded with PSB consortium assembly for SC.

4.2. *In vivo interaction between PSB and nHAs on maize growth, nutrient uptake, and P-use efficiency*

Our first hypothesis of synergies between SnHAs and PSB was partially confirmed by maize growth and nutrient uptake (Table 2; Table 3). Indeed, in terms of root and total plant growth, as well as P and K uptake, the combined application of SnHAs (+S) and PSB seed coating (SC) had a greater impact compared to the sole application of SnHAs. However, the +S SC treatment did not outperform the PSB inoculation alone (SC and BR), and similar plant parameters were reported when SnHAs was applied alone (+S NB) compared to no application of nHAs (−S NB). Similar to our results on SnHAs in comparison with no application, no significant variation was observed on the root growth of cornsalad (*Valeriana locusta*) treated with fish-bones nanoparticles (Adamiano et al., 2021). However, contrary to our results, decreases in shoot dry weight were found on cornsalad (Adamiano et al., 2021), and a beneficial effect of the sole application of biogenic nHAs was reported on root and total plant biomass of barley (Pilotto et al., 2024). Concerning synergies between PSB and nHAs, *Pseudomonas alloputida* co-applied with nHAs did not show any enhanced combined effect on barley growth and nutrients compared to the PSB applied alone under fertilized controls (Pilotto et al., 2024). This inconsistency with the synergism we observed for total plant biomass may be due to the use of a single strain instead of a PSB consortium. In addition, *P. alloputida* was not screened either for IAA production which is known to promote root growth or for N_2 fixation. Additionally, no synergism was observed on soybean shoot and root biomass when *Bacillus velezensis*, reported to be a good P solubilizer (Saxena et al., 2020), was co-applied with HA in lime and no-lime soils, characterized by alkaline and acidic pH (C. Li et al., 2021; X.L. Li et al., 2021). Nevertheless the application of nHAs with *B. velezensis* SC in combination with a fungicide synergistically promoted soybean plant growth. This was explained by the capacity of the fungicide to inhibit the competition between the inoculated *Bacillus* and some fungi, allowing, similarly to our experiment, an optimal environment for bacterial growth and functioning. Consistently in non-sterile soil, it was demonstrated that when urea-nHAs was co-applied with PSB, such as *Bacillus megaterium* or *Pseudomonas aeruginosa*, it remarkably promoted hemp plant growth compared with the sole application of urea-nHAs or single PSB (Vadhel et al., 2023), thus supporting a synergism between treatments. The synergism we observed between SnHAs and SC on the root and total plant P content (Table 3) proved the significant role of PSB consortia in the dissolution of weakly soluble P forms, such as nHAs, and highlighted for the first time the efficacy of SC

to enhance P solubilization from nanoparticles. Concerning the combined effect of HA (nano)particles and PSB on plant P uptake, only a few studies have been conducted (Meyer et al., 2017; Pilotto et al., 2024), and none have applied microbial consortia. Pilotto et al. (2024) found that the combined application of nHAs with *P. alloputida* did not determine a synergistic effect on barley P concentration and content in both roots and shoots. Accordingly, in calcareous soil, the combination of *P. protegens* and ^{33}P-labeled synthetic HA did not synergistically enhance wheat P uptake, either in non-sterilized or sterilized soil (Meyer et al., 2017). The lack of synergism, with respect to our results (Table 3), can be attributed to high soil pH of the substrates used in other experiments, which can limit the availability of P from HA, thereby reducing the effectiveness of bacterial inoculation, or to the efficiency of the selected PSB strains. Moreover, the inoculum density might have led to a competition of nutrients among microbes (Meyer et al., 2017; Mawarda et al., 2020), leading to a decline in the beneficial effect on plant P uptake. This could also explain why in our study the addition to the substrate of a PSB reinforcement failed to deliver synergisms on maize growth and nutrient uptake, compared to the lower bacterial cell density characterizing SC (Table 2; Table 3).

The significant increase of PUE and PRE observed with PSB coating and salmon-derived nHAs (Fig. 4a,b) strongly supports the potential environmental benefits of the system (Veneklaas et al., 2012). Our results indicated for the first time the potential role of PSB consortia in enhancing the amount of total biomass of maize that is produced per unit of P taken up from SnHAs. Indeed, a previous study on barley, in which a single species of PSB was applied with nHAs, found higher soil P availability when compared to the sole application of nHAs, but no significant differences in plant P uptake (Pilotto et al., 2024). The unique study that invested P use efficiency found greater PUE in tomato when nano-rock phosphate and a single species of PSB were applied with respect to not-inoculated controls (Yasmeen et al., 2022).

Similar to P, K content was synergistically increased by the interactions of the two factors, SnHAs and PSB (Table 3). Certain PSB species exhibit the ability to solubilize both P and K, including *Pseudomonas* and *Paraburkholderia* species, used as inoculants in our consortium (Han and Lee, 2006; Tian et al., 2024; Zhang et al., 2024). This ability was strongly linked to the production of OAs. Therefore, our PSB consortium facilitated the simultaneous uptake of both P and K, indicating the multifaceted beneficial traits of the strains in the *in vivo* system.

Inorganic P acquisition is facilitated by both plant secretion of acid phosphatases in soil and by the induction of high-affinity P transporters (Smith et al., 2003; Li et al., 2004). Among the five *PHT* transporter families (*PHT1, PHT2, PHT3, PHT4* and *PHT5*), in maize the *PHT1* family comprises 13 high-affinity transporters (*PHT1;1-1;13*) (Liu et al., 2015), which are strongly expressed at the root-soil interface, including root hairs (Nagy et al., 2006; Nussaume et al., 2011; López-Arredondo et al., 2014; Lambers and Plaxton, 2015). In our study, four out of six P-related genes were differentially upregulated by the treatments (Fig. 5). The activation of *PHT1* transporters was widely studied in response to mycorrhizal inoculation (Loth-Pereda et al., 2011; Tian et al., 2013; Sawers et al., 2017), as well as to PSB, although to a lesser extent (Srivastava and Srivastava, 2020; Alzate Zuluaga et al., 2021). Our results demonstrated that SnHAs, alone or in combination with PSB treatments, with both SC and BR, exerted a great contribution to upregulating P transporters, especially in *PHT1;1, PHT1;2, PHT1;4* and *PHT1;6*. Nevertheless, the role of PSB alone, particularly BR treatment, was more evident than SC (*i.e.*, *PHT1;2, PHT1;4, PHT1;6*). These results are partially consistent with the findings on maize growth and P uptake, unravelling the complex regulatory mechanisms of the interactions between SnHAs and PSB. Interestingly, the expression of *PHT1;5,* although it was not significantly affected by treatments, appears to be inhibited compared to the control, showing a mean decrease of −50 % across all the treatments. Similar results were reported by Alzate Zuluaga et al. (2021) who found that the expression of *PHT1;5* in maize was downregulated by the inoculation of *Enterobacter* strain 15S compared to uninoculated plants. They observed that *PHT1;5* tended to decrease its expression in inoculated plants, regardless of soil P availability. This implies that the reduction might not be due to changes in P uptake after bacterial inoculation, but rather to plant response to the association with the bacteria. In addition, the P acquisition we observed in our study can also be regulated by members of other *PHT* families, such as *PHT2, PHT3, PHT4 and PHT5* (Wang et al., 2017). No significant differences in *ACP1* gene expression were observed between treatments and control. However, despite the lack of statistical significance, we could detect some trends in gene regulation across treatments. For example, with the co-application of SnHAs and PSB, a decrease of 12 % in *ACP1* expression was observed, while with SnHAs or PSB alone its expression increased (+30 % and +10 %, respectively). Since acid phosphatase production is an alternative strategy for plants to cope with P deficiency (Zhang et al., 2023), the reduced expression of *ACP1* in +S SC and +S BR treatments may suggest an adequate P status in maize plants.

4.3. Effect of SC on the establishment and growth of PSB in plant-soil system

To test our second hypothesis, we evaluated the effectiveness of SC in promoting the establishment and growth of PSB in the plant-soil system. We hypothesized that SC alone would be sufficient to support the bacterial growth in the substrate and roots, leading to an efficient inoculum establishment without the need for additional BR. Indeed, soil re-inoculation is typically more expensive in large-scale applications because it requires specialized equipment, larger volumes of inoculants, and higher storage and transportation costs, making it more expensive than SC (O'Callaghan, 2016; Rocha et al., 2019). To maintain the bacterial threshold and survival, and prevent inoculant loss, we used CMC as an adhesive, ensuring stable inoculation and promoting consistent root colonization and microbial growth, as suggested by Bashan et al. (2014). The strains included in the PSB consortium exhibit endophytic competence (Phillips et al., 2008; Poosakkannu et al., 2015; Vio et al., 2020), making SC a suitable technique to introduce these beneficial microorganisms directly into the rhizosphere with the potential to colonize roots. In our study, SC without SnHAs increased the bacterial biomass in the substrate, suggesting that coating effectively delivered the PSB strains, which thrived in the environment (Fig. 6). However, within the roots, bacterial biomass was higher in the BR treatments, and there was a clear correlation between increasing bacterial inoculum density and higher root bacterial biomass. Nevertheless, looking at the global pattern of the treatments (Fig. 4c), both root and substrate bacterial biomass were strongly associated with the +S SC treatment, suggesting that SC efficiently promoted bacterial growth and persistence. These findings indicated that SC was sufficient for enriching bacterial biomass in the substrate and for enhancing root colonization, after 34 days of maize growth in microcosm, without the need for bacterial re-inoculation.

4.4. Linking in vitro and in vivo studies on PSB and nHA substrates to disclose the mechanisms of P solubilization and related plant performance

Our results demonstrated a strong functional linkage between the activity of the PSB consortium used as SC and maize performance, emphasizing the role of OAs and solubilization efficiency in plant nutrient acquisition and gene expression regulation. The clear relationship between *in vitro* solubilization patterns and *in vivo* plant growth (as displayed in the PCoA plots, Fig. 7a,b) further supports this connection, suggesting that the microbial activity measured under laboratory conditions is a strong predictor of plant performance under real conditions. Propionic acid and solubilization efficiency at the latest time of sampling were the most influential predictors of plant functionality and this reveals the importance of specific OAs in mediating P availability and plant uptake efficiency. Previously, citric acid was found to

be the best predictor for P solubilization from nHAs (Wang et al., 2016; Monroy Miguel et al., 2020). Thus, the detection of specific OAs might be predictive of high P solubilization efficiency and P uptake by plant when combining efficient PSB and nHAs. The PCoA biplot (Fig. 7a,b) revealed that most *in vitro* parameters positively correlated with plant growth and nutrient uptake, indicating that PSB-driven phosphate solubilization enhances maize performance. However, fumaric and tartaric acids exhibited an opposite trend, suggesting these OAs do not contribute to enhanced nutrient assimilation and plant growth. Instead, their positive correlation with plant P gene expression could indicate an alternative regulatory role, possibly linked to metabolic shifts in plant-microbe interactions, as described by Rosier et al. (2018) studying biochemical network in plant-PSB interactions. These findings provide strong evidence that specific microbial metabolic traits, especially solubilization efficiency and OA secretion, can drive plant functional responses.

5. Conclusions

The results of our study demonstrated that co-applying phosphate-based materials from food industry residues (*i.e.* salmon bones) SnHAs and PSB SC synergistically enhanced maize root growth and total plant biomass compared with nHAs applied alone. In terms of nutrient uptake, our findings highlighted the synergisms between SnHAs and SC on P content, and the efficiency of the PSB consortium in solubilizing weakly soluble P forms, such as nHAs. Indeed, P-use efficiency and recovery increased with SnHAs and SC with by 25 % and three-fold, respectively, compared to SnHAs alone and SnHAs with bacterial reinforcement (BR). Maize P uptake declined when co-applying SnHAs with BR, likely due to higher inoculum density causing nutrient competition among microbes and reducing beneficial effects on P uptake. We also found that the total bacterial biomass in both root and substrate was closely related to SC plus SnHAs. Thus, consistently with our hypothesis SC could efficiently promote bacterial establishment without additional inoculation. Finally, we demonstrated that propionic acid production and P-solubilization efficiency of PSB co-applied with nHAs are key drivers of maize growth and P uptake. Additionally, SC with SnHAs strongly promoted maize growth and P uptake while downregulating P-related genes compared to SnHAs alone. This demonstrates that in absence of PSB, the plant activates P transporter genes to counteract P starvation. Therefore, the co-application of SnHAs and SC provides a promising sustainable strategy to enhance crop productivity and P-use efficiency by exploiting fish industry residues, while minimizing inoculant density. Future studies should explore the application of SnHAs and SC in non-sterilized soils to assess their interactions with resident microbial communities, and testing their feasibility in soils across different climates. Lastly, a broader study on plant transcriptomic response is needed to identify the involved biological, molecular, and metabolic mechanisms.

CRediT authorship contribution statement

Piera Quattrocelli: Writing – review & editing, Writing – original draft, Visualization, Validation, Methodology, Investigation, Formal analysis, Data curation, Conceptualization. **Clara Piccirillo:** Writing – review & editing, Methodology. **Eiko E. Kuramae:** Writing – review & editing. **Robert C. Pullar:** Writing – review & editing. **Laura Ercoli:** Writing – review & editing, Supervision. **Elisa Pellegrino:** Writing – review & editing, Writing – original draft, Visualization, Supervision, Resources, Methodology, Investigation, Funding acquisition, Data curation, Conceptualization.

Funding

This work was funded by the European Agricultural Fund for Rural Development 2004–2020 for Tuscany (Italy) mis. 16.2 "MICROforAGRI – MICRorganismi ed idrOssiapatatite da sOttoprodotti della lavorazione del pesce come Risorsa di fosforo in AGRIcoltura sostenibile" (CUP ART€A 1074061 – CUP CIPE J53C23002020002; Principal investigator: E. Pellegrino). Piera Quattrocelli was supported by a PhD scholarship in Agrobiosciences (XXXVII cycle) from the Scuola Superiore Sant'Anna (SSSA, Pisa, Italy).

Declaration of competing interest

The authors declare that they have no known competing financial interests or personal relationships that could have influenced the work reported in this paper.

Acknowledgments

The authors thank Mare Aperto SRL for providing the tuna bones, Irene Nicolini and Francesco Pompilii for providing help in the set-up of the *in vivo* experimental system and sample collection, and Dr. Francesca Scalera for SEM analysis.

Appendix A. Supplementary data

Supplementary data to this article can be found online at https://doi.org/10.1016/j.scitotenv.2025.179082.

Data availability

Data will be made available on request.

References

Abdelmigid, H.M., Morsi, M.M., Hussien, N.A., Alyamani, A.A., Alhuthal, N.A., Albukhaty, S., 2022. Green synthesis of phosphorous-containing hydroxyapatite nanoparticles (nHAP) as a novel nano-fertilizer: preliminary assessment on pomegranate (*Punica granatum* L.). Nanomaterials 12, 1527. https://doi.org/10.3390/nano12091527.

Adamiano, A., Fellet, G., Vuerich, M., Scarpin, D., Carella, F., Piccirillo, C., Jeon, J.R., Pizzutti, A., Marchiol, L., Iafisco, M., 2021. Calcium phosphate particles coated with humic substances: a potential plant biostimulant from circular economy. Molecules 26, 2810. https://doi.org/10.3390/molecules26092810.

Alori, E.T., Glick, B.R., Babalola, O.O., 2017. Microbial phosphorus solubilization and its potential for use in sustainable agriculture. Front. Microbiol. 8, 971. https://doi.org/10.3389/fmicb.2017.00971.

Alzate Zuluaga, M.Y., Martinez de Oliveira, A.L., Valentinuzzi, F., Tiziani, R., Pii, Y., Mimmo, T., Cesco, S., 2021. Can inoculation with the bacterial biostimulant *Enterobacter* sp. strain 15S be an approach for the smarter P fertilization of maize and cucumber plants? Front. Plant Sci. 12, 719873. https://doi.org/10.3389/fpls.2021.719873.

Anderson, M., Gorley, R.N., Clarke, K.R., 2008. PERMANOVA+ for PRIMER: Guide to Software and Statistical Methods. Primer-E Limited, Auckland, New Zealand.

Azam, H.M., Alam, S.T., Hasan, M., Yameogo, D.D.S., Kannan, A.D., Rahman, A., Kwon, M.J., 2019. Phosphorous in the environment: characteristics with distribution and effects, removal mechanisms, treatment technologies, and factors affecting recovery as minerals in natural and engineered systems. Environ. Sci. Pollut. Res. 26, 20183–20207. https://doi.org/10.1007/s11356-019-04732-y.

Bashan, Y., Kamnev, A.A., de Bashan, L.E., 2013a. Tricalcium phosphate is inappropriate as a universal selection factor for isolating and testing phosphate-solubilizing bacteria that enhance plant growth: a proposal for an alternative procedure. Biol. Fertil. Soils 49, 465–479. https://doi.org/10.1007/s00374-012-0737-7.

Bashan, Y., Kamnev, A.A., de Bashan, L.E., 2013b. A proposal for isolating and testing phosphate-solubilizing bacteria that enhance plant growth. Biol. Fertil. Soils 49, 1–2. https://doi.org/10.1007/s00374-012-0756-4.

Bashan, Y., de Bashan, L.E., Prabhu, S.R., Hernandez, J.P., 2014. Advances in plant growth-promoting bacterial inoculant technology: formulations and practical perspectives. Plant Soil 378, 1–33. https://doi.org/10.1007/s11104-013-1956-x.

Batista, B.D., Bonatelli, M.L., Quecine, M.C., 2021. Fast screening of bacteria for plant growth promoting traits. In: The Plant Microbiome: Methods and Protocols. Springer, Beerlin, Germany, pp. 61–75. https://doi.org/10.1007/978-1-0716-1040-4_7.

Carella, F., Seck, M., Degli Esposti, L., Diadiou, H., Maienza, A., Baronti, S., Vignaroli, P., Vaccari, F.P., Iafisco, M., Adamiano, A., 2021. Thermal conversion of fish bones into fertilizers and biostimulants for plant growth - a low tech valorization process for the development of circular economy in least developed countries. J. Environ. Chem. Eng. 9, 104815. https://doi.org/10.1016/j.jece.2020.104815.

Carpenter, S.R., 2005. Eutrophication of aquatic ecosystems: Bistability and soil phosphorus. Proc. Natl. Acad. Sci. USA 102, 10002–10005. https://doi.org/10.1073/pnas.050395910.

Carpenter, S.R., Bennett, E.M., 2011. Reconsideration of the planetary boundary for phosphorus. Environ. Res. Lett. 6, 014009. https://doi.org/10.1088/1748-9326/6/1/014009.
Chen, Y.P., Rekha, P.D., Arun, A.B., Shen, F.T., Lai, W.A., Young, C.C., 2006. Phosphate solubilizing bacteria from subtropical soil and their tricalcium phosphate solubilizing abilities. Appl. Soil Ecol. 34, 33–41. https://doi.org/10.1016/j.apsoil.2005.12.002.
Clarke, K.R., Gorley, R.N., 2015. Getting Started With PRIMER v7. PRIMER-E, Plymouth Marine Laboratory, Plymouth, UK.
Clarke, K.R., Warwick, R.M., 2001. Change in Marine Communities: An Approach to Statistical Analysis and Interpretation (PRIMER-E). Plymouth Marine Laboratory, Plymouth, UK.
Clarke, K.R., Somerfield, P.J., Gorley, R.N., 2008. Testing of null hypotheses in exploratory community analyses: similarity profiles and biota-environment linkage. J. Exp. Mar. Biol. Ecol. 366, 56–69. https://doi.org/10.1016/j.jembe.2008.07.009.
Cortés-Rojas, D., Beltrán-Acosta, C., Zapata-Narvaez, Y., Chaparro, M., Gómez, M., Cruz Barrera, M., 2021. Seed coating as a delivery system for the endophyte *Trichoderma koningiopsis* Th003 in rice (*Oryza sativa*). Appl. Microbiol. Biotechnol. 105, 1889–1904. https://doi.org/10.1007/s00253-021-11146-9.
Cumpa-Velásquez, L.M., Moriconi, J.I., Dip, D.P., Castagno, L.N., Puig, M.L., Maiale, S.J., Santa-María, G.E., Sannazzaro, A.I., Estrella, M.J., 2021. Prospecting phosphate solubilizing bacteria in alkaline-sodic environments reveals intra-specific variability in *Pantoea eucalypti* affecting nutrient acquisition and rhizobial nodulation in *Lotus tenuis*. Appl. Soil Ecol. 168, 104125. https://doi.org/10.1016/j.apsoil.2021.104125.
de Bang, T.C., Husted, S., Laursen, K.H., Persson, D.P., Schjoerring, J.K., 2021. The molecular-physiological functions of mineral macronutrients and their consequences for deficiency symptoms in plants. New Phytol. 229, 2446–2469. https://doi.org/10.1111/nph.17074.
Delvasto, P., Valverde, A., Ballester, A., Igual, J.M., Muñoz, J.A., González, F., Blázquez, M.L., García, C., 2006. Characterization of brushite as a re-crystallization product formed during bacterial solubilization of hydroxyapatite in batch cultures. Soil Biol. Biochem. 38, 2645–2654. https://doi.org/10.1016/j.soilbio.2006.03.020.
do Amaral Leite, A., de Souza Cardoso, A.A., de Almeida Leite, R., Barrera, A.M.V., Queiroz, D.D.L., Viana, T.C., de Oliveira-Longatti, S.M., Silva, C.A., de Souza Moreira, F.M., Lehmann, J., Melo, L.C.A., 2024. Phosphate-solubilizing bacteria increase maize phosphorus uptake from magnesium-enriched poultry manure biochar. Biol. Fertil. Soils 60, 421–436. https://doi.org/10.1007/s00374-024-01808-x.
Dorozhkin, S.V., 2010. Calcium orthophosphate bioceramics. J. Biomater. Tissue Eng. 5, 57–100. https://doi.org/10.1016/j.biomaterials.2009.11.050.
Dorozhkin, S.V., 2012. Dissolution mechanism of calcium apatites in acids: a review of literature. World J. Methodol. 2, 1 https://doi.org/0.5662/wjm.v2.i.
Dorozhkin, S.V., Epple, M., 2002. Biological and medical significance of calcium phosphates. Angew. Chem. Int. Ed. 41, 3130–3146. https://doi.org/10.1002/1521-3773(20020902)41:17<3130::AID-ANIE3130>3.0.CO;2-1.
Dupas, R., Delmas, M., Dorioz, J.M., Garnier, J., Moatar, F., Gascuel-Odoux, C., 2015. Assessing the impact of agricultural pressures on N and P loads and eutrophication risk. Ecol. Indic. 48, 396–407. https://doi.org/10.1016/j.ecolind.2014.08.007.
Ebrahimi, M., Botelho, M.G., Dorozhkin, S.V., 2017. Biphasic calcium phosphates biocer amics (HA/TCP): concept, physicochemical properties, and the impact of standardization of study protocols in biomaterials research. Mater. Sci. Eng. 71, 1293–1312. https://doi.org/10.1016/j.msec.2016.11.039.
Emami, S., Alikhani, H.A., Pourbabaee, A.A., Etesami, H., Motasharezadeh, B., Sarmadian, F., 2020. Consortium of endophyte and rhizosphere phosphate solubilizing bacteria improves phosphorous use efficiency in wheat cultivars in phosphorus deficient soils. Rhizosphere 14, 100196. https://doi.org/10.1016/j.rhisph.2020.100196.
Farhat, M.B., Boukhris, I., Chouayekh, H., 2015. Mineral phosphate solubilization by *Streptomyces* sp. CTM396 involves the excretion of gluconic acid and is stimulated by humic acids. FEMS Microbiol. Lett. 362, fnv008. https://doi.org/10.1093/femsle/fnv008.
Feng, S., Zeng, W., Luo, F., Zhao, J., Yang, Z., Sun, Q., 2010. Antibacterial activity of organic acids in aqueous extracts from pine needles (*Pinus massoniana* Lamb.). Food Sci. Biotechnol. 19. https://doi.org/10.1007/s10068-010-0005-2, 35 41.
Fierer, N., Jackson, J.A., Vilgalys, R., Jackson, R.B., 2005. Assessment of soil microbial community structure by use of taxon specific quantitative PCR assays. Appl. Environ. Microbiol. 71 (4117), 4120. https://doi.org/10.1128/AEM.71.7.4117-4120.2005.
Gardes, M., Bruns, T.D., 1993. ITS primers with enhanced specificity for basidiomycetes application to the identification of mycorrhizae and rusts. Mol. Ecol. 2, 113–118. https://doi.org/10.1111/j.1365-294X.1993.tb00005.x.
Gogos, A., Knauer, K., Bucheli, T.D., 2012. Nanomaterials in plant protection and fertilization: current state, foreseen applications, and research priorities. J. Agric. Food Chem. 60, 9781–9792. https://doi.org/10.1021/jf302154y.
Gómez-Muñoz, B., Jensen, L.S., De Neergaard, A., Richardson, A.E., Magid, J., 2018. Effects of *Penicillium bilaii* on maize growth are mediated by available phosphorus. Plant Soil 431, 159–173. https://doi.org/10.1007/s11104-018-3756-9.
Hameeda, B., Reddy, Y.H.K., Rupela, O.P., Kumar, G.N., Reddy, G., 2006. Effect of carbon substrates on rock phosphate solubilization by bacteria from composts and macrofauna. Curr. Microbiol. 53, 298–302. https://doi.org/10.1007/s00284-006-0004-y.
Han, H.S., Lee, K.D., 2006. Effect of co-inoculation with phosphate and potassium solubilizing bacteria on mineral uptake and growth of pepper and cucumber. Plant Soil Environ. 52, 130–137. https://doi.org/10.17221/3356-PSE.
Hanway, J.J., 1963. Growth stages of corn (*Zea mays*, L.). Agron. J. 55, 487–492. https://doi.org/10.2134/agronj1963.00021962005500050024x.
Haskett, T.L., Tkacz, A., Poole, P.S., 2021. Engineering rhizobacteria for sustainable agriculture. ISME J. 15, 949–964. https://doi.org/10.1038/s41396-020-00835-4.
Hassani, M.A., Durán, P., Hacquard, S., 2018. Microbial interactions within the plant holobiont. Microbiome 6, 1–17. https://doi.org/10.1186/s40168-018-0445-0.
Hazarika, A., Yadav, M., Yadav, D.K., Yadav, H.S., 2022. An overview of the role of nanoparticles in sustainable agriculture. Biocatal. Agric. Biotechnol. 43, 102399. https://doi.org/10.1016/j.bcab.2022.102399.
Hedley, M., McLaughlin, M., 2005. Reactions of phosphate fertilizers and by-products in soils. In: Phosphorus: Agriculture and the Environment, American Society of Agronomy, Inc., Crop Science Society of America, Inc., Soil Science Society of America, Inc., Agronomy Monographs, USA, pp. 181–252.
Herrera-Estrella, L., López-Arredondo, D., 2016. Phosphorus: the underrated element for feeding the world. Trends Plant Sci. 21, 461–463. https://doi.org/10.1016/j.tplants.2016.04.010.
Hoagland, D.R., Arnon, D.I., 1950. The water-culture method for growing plants without soil. Calif. Agric. Exp. Stn. Circ. 347, 1–32.
Hsu, P.C.L., O'Callaghan, M., Condron, L., Hurst, M.R., 2018. Use of a gnotobiotic plant assay for assessing root colonization and mineral phosphate solubilization by *Paraburkholderia bryophila* Ha185 in association with perennial ryegrass (*Lolium perenne* L.). Plant Soil 425, 43–55. https://doi.org/10.1007/s11104-018-3633-6.
Hu, J., Yang, T., Friman, V.P., Kowalchuk, G.A., Hautier, Y., Li, M., Wei, Z., Xu, Y., Shen, Q., Jousset, A., 2021. Introduction of probiotic bacterial consortia promotes plant growth via impacts on the resident rhizosphere microbiome. Proc. R. Soc. 288, 2021396. https://doi.org/10.1098/rspb.2021.1396.
Illmer, P., Schinner, F., 1995. Solubilization of inorganic calcium phosphates-solubilization mechanisms. Soil Biol. Biochem. 27, 257–263. https://doi.org/10.1016/0038-0717(94)00190-C.
Irabor, A., Mmbaga, M.T., 2017. Evaluation of selected bacterial endophytes for biocontrol potential against *Phytophthora* blight of bell pepper (*Capsicum annuum* L.) J. Plant. Pathol. Microbiol. 28. https://doi.org/10.4172/2157-7471.1000424, 31 34.
ISTA, 2023. International Rules for Seed Testing. International Seed Testing Association, Wallisellen, Switzerland.
Jia, X., Shi, N., Tang, W., Su, Z., Chen, H., Tang, Y., Sun, B., Zhao, L., 2022. Nano-hydroxyapatite increased soil quality and boosted beneficial soil microbes. Plant Nano Biol. 1, 100002. https://doi.org/10.1016/j.plana.2022.100002.
Khan, S.T., 2022. Consortia-based microbial inoculants for sustaining agricultural activities. Appl. Soil Ecol. 176, 104503. https://doi.org/10.1016/j.apsoil.2022.104503.
Kooshki, M.J., Haghighi, M., 2024. Enhancing tomato growth, quality, and yield through the application of bio and nano-bio phosphorus in conjunction with Pseudomonas putida inoculation. J. Agric. Food Res. 18, 101483. https://doi.org/10.1016/j.jafr.2024.101483.
Kumar, P., Pandey, P., Dubey, R.C., Maheshwari, D.K., 2016. Bacteria consortium optimization improves nutrient uptake, nodulation, disease suppression and growth of the common bean (*Phaseolus vulgaris*) in both pot and field studies. Rhizosphere 2, 13–23. https://doi.org/10.1016/j.rhisph.2016.09.002.
Lambers, H., Plaxton, W.C., 2015. Phosphorus: back to the roots, in. Annu. Plant Rev. 48, 1–22. https://doi.org/10.1002/9781118958841.ch1 phosphorus metabolism in plants.
Lane, D., 1991. 16s/23s rRNA sequencing. In: Nucleic Acid Techniques in Bacterial Systematics. John Wiley & Sons, New York, pp. 115–175.
Larsen, S., 1966. Solubility of hydroxyapatite. Nature 212, 605.
Li, C., Rippner, D.A., Manavalan, L.P., Parikh, S.J., 2021a. Evaluation of *Bacillus* seed coatings on soybean phosphorus uptake in an oxisol fertilized with ^{32}P-labeled hydroxyapatite. Plant Soil 464, 273–287. https://doi.org/10.1007/s11104-021-04941-w.
Li, S.M., Li, L., Zhang, F.S., Tang, C., 2004. Acid phosphatase role in chickpea/maize intercropping. Ann. Bot. 94, 297–303. https://doi.org/10.1093/aob/mch140.
Li, X.L., Zhao, X.Q., Dong, X.Y., Ma, J.F., Shen, R.F., 2021b. Secretion of gluconic acid from *Nguyenibacter* sp. L1 is responsible for solubilization of aluminum phosphate. Front. Microbiol. 12, 784025. https://doi.org/10.3389/fmicb.2021.784025.
Liu, R., Lal, R., 2014. Synthetic apatite nanoparticles as a phosphorus fertilizer for soybean(*Glycine max*). Sci. Rep. UK 4, 5686. https://doi.org/10.1038/srep05686.
Liu, R., Lal, R., 2015. Potentials of engineered nanoparticles as fertilizers for increasing agronomic productions. Sci. Total Environ. 514, 131–139. https://doi.org/10.1016/j.scitotenv.2015.01.104.
Liu, X., Mei, S., Salles, J.F., 2023. Inoculated microbial consortia perform better than single trains in living soil: a meta-analysis. Appl. Soil Ecol. 190, 105011. https://doi.org/10.1016/j.apsoil.2023.105011.
Liu, Z., Li, Y.C., Zhang, S., Fu, Y., Fan, X., Patel, J.S., Zhang, M., 2015. Characterization of phosphate-solubilizing bacteria isolated from calcareous soils. Appl. Soil Ecol. 96, 217–224.
Livak, K.J., Schmittgen, T.D., 2001. Analysis of relative gene expression data using real-time quantitative PCR and the $2^{-\Delta\Delta CT}$ method. Methods 25, 402–408. https://doi.org/10.1006/meth.2001.1262.
López-Arredondo, D.L., Leyva-González, M.A., González-Morales, S.I., López-Bucio, J., Herrera-Estrella, L., 2014. Phosphate nutrition: improving low-phosphate tolerance in crops. Ann. Rev. Plant Biol. 65, 95–123. https://doi.org/10.1146/annurev-arplant-050213-035949.
Loth-Pereda, V., Orsini, E., Courty, P.E., Lota, F., Kohler, A., Diss, L., Blaudez, D., Chalot, M., Nehls, U., Bucher, M., Martin, F., 2011. Structure and expression profile of the phosphate Pht1 transporter gene family in mycorrhizal *Populus trichocarpa*. Plant Physiol. 156, 2141–2154. https://doi.org/10.1104/pp.111.180646.
Ma, Y., 2019. Seed coating with beneficial microorganisms for precision agriculture. Biotechnol. Adv. 37, 107423. https://doi.org/10.1016/j.biotechadv.2019.107423.

Mahbubul, I.M., Elcioglu, E.B., Amalina, M.A., Saidur, R.J.P.T., 2019. Stability, thermophysical properties and performance assessment of alumina–water nanofluid with emphasis on ultrasonication and storage period. Powder Technol. 345, 668–675. https://doi.org/10.1016/j.powtec.2019.01.041.

Manzoor, M., Abbasi, M.K., Sultan, T., 2017. Isolation of phosphate solubilizing bacteria from maize rhizosphere and their potential for rock phosphate solubilization–mineralization and plant growth promotion. Geomicrobiol J. 34, 81–95. https://doi.org/10.1080/01490451.2016.1146373.

Martinez Arbizu, P., 2020. pairwiseAdonis: Pairwise Multilevel Comparison Using Adonis. R Package Version 0.4.

Mawarda, P.C., Le Roux, X., Van Elsas, J.D., Salles, J.F., 2020. Deliberate introduction of invisible invaders: a critical appraisal of the impact of microbial inoculants on soil microbial communities. Soil Biol. Biochem. 148, 107874. https://doi.org/10.1016/j.soilbio.2020.107874.

Meyer, G., Bünemann, E.K., Frossard, E., Maurhofer, M., Mäder, P., Oberson, A., 2017. Gross phosphorus fluxes in a calcareous soil inoculated with *Pseudomonas protegens* CHA0 revealed by ^{33}P isotopic dilution. Soil Biol. Biochem. 104, 81–94. https://doi.org/10.1016/j.soilbio.2016.10.001.

Minchev, Z., Kostenko, O., Soler, R., Pozo, M.J., 2021. Microbial consortia for effective biocontrol of root and foliar diseases in tomato. Front. Plant Sci. 12, 756368. https://doi.org/10.3389/fpls.2021.756368.

Mollier, A., Pellerin, S., 1999. Maize root system growth and development as influenced by phosphorus deficiency. J. Exp. Bot. 50, 487–497. https://doi.org/10.1093/jxb/50.333.487.

Monroy Miguel, R., Carrillo González, R., Rios Leal, E., González-Chávez, M.D.C.A., 2020. Screening bacterial phosphate solubilization with bulk-tricalcium phosphate and hydroxyapatite nanoparticles. A. Van. Leeuw. J. Microb. 113, 1033–1047. https://doi.org/10.1007/s10482-020-01409-2.

Montalvo, D., McLaughlin, M.J., Degryse, F., 2015. Efficacy of hydroxyapatite nanoparticles as phosphorus fertilizer in andisols and oxisols. Soil Sci. Soc. Am. J. 79, 551–558. https://doi.org/10.2136/sssaj2014.09.0373.

Muyzer, G., De Waal, E.C., Uitterlinden, A., 1993. Profiling of complex microbial population by denaturing gradient gel electrophoresis analysis of polymerase chain reaction-amplified genes coding for 16S rRNA. Appl. Environ. Microbiol. 59, 695–700. https://doi.org/10.1128/aem.59.3.695-700.1993.

Nagy, R., Vasconcelos, M.J.V., Zhao, S., McElver, J., Bruce, W., Amrhein, N., Raghothama, K.G., Bucher, M., 2006. Differential regulation of five PHT1 phosphate transporters from maize (*Zea mays* L.). Plant Biol. 8, 186–197. https://doi.org/10.1055/s-2005-873052.

Nair, R., Varghese, S.H., Nair, B.G., Maekawa, T., Yoshida, Y., Kumar, D.S., 2010. Nanoparticulate material delivery to plants. Plant Sci. 179, 154–163. https://doi.org/10.1016/j.plantsci.2010.04.012.

Nussaume, L., Kanno, S., Javot, H., Marin, E., Pochon, N., Ayadi, A., Nakanishi, T.M., Thibaud, M.C., 2011. Phosphate import in plants: focus on the PHT1 transporters. Front. Plant Sci. 2, 83. https://doi.org/10.3389/fpls.2011.00083.

O'Callaghan, M., 2016. Microbial inoculation of seed for improved crop performance: issues and opportunities. Appl. Microbiol. Biotechnol. 100, 5729–5746. https://doi.org/10.1007/s00253-016-7590-9.

Oksanen, J., Blanchet, F.G., Friendly, M., Kindt, R., Legendre, P., McGlinn, D., Minchin, P.R., O'Hara, R.B., Simpson, G.L., Solymos, P., Henry, M., Stevens, H., Szoecs, E., Wagner, H., 2020. Vegan Community Ecology Package Version 2.5-7 November 2020. R Project for Statistical Computing, Vienna, Austria.

Pan, H., Darvell, B.W., 2010. Effect of carbonate on hydroxyapatite solubility. Cryst. Growth Des. 10, 845–850. https://doi.org/10.1021/cg901199h.

Panagos, P., Köningner, J., Ballabio, C., Liakos, L., Muntwyler, A., Borrelli, P., Lugato, E., 2022. Improving the phosphorus budget of European agricultural soils. Sci. Total Environ. 853, 158706. https://doi.org/10.1016/j.scitotenv.2022.158706.

Pérez-Rodriguez, M.M., Piccoli, P., Anzuay, M.S., Baraldi, R., Neri, L., Taurian, T., Lobato Ureche, M.A., Segura, D.M., Cohen, A.C., 2020. Native bacteria isolated from roots and rhizosphere of *Solanum lycopersicum* L. increase tomato seedling growth under a reduced fertilization regime. Sci. Rep. UK 10, 15642.

Phillips, L.A., Germida, J.J., Farrell, R.E., Greer, C.W., 2008. Hydrocarbon degradation potential and activity of endophytic bacteria associated with prairie plants. Soil Biol. Biochem. 40, 3054–3064. https://doi.org/10.1016/j.soilbio.2008.09.006.

Piccirillo, C., Pullar, R.C., Tobaldi, D.M., Castro, P.L., Pintado, M.E., 2014. Hydroxyapatite and chloroapatite derived from sardine by-products. Ceram. Int. 40, 13231–13240. https://doi.org/10.1016/j.ceramint.2014.05.030.

Pii, Y., Alessandrini, M., Dall'Osto, L., Guardini, K., Prinsi, B., Espen, L., Zamboni, A., Varanini, Z., 2016. Time-resolved investigation of molecular components involved in the induction of NO_3^- high affinity transport system in maize roots. Front. Plant Sci. 7, 1657. https://doi.org/10.3389/fpls.2016.01657.

Pilotto, L., Zuluaga, M.Y.A., Scalera, F., Piccirillo, C., Marchiol, L., Civilini, M., Pii, J., Cesco, S., Fellet, G., 2024. Sustainable crop fertilization by combining biogenic nano hydroxyapatite and P solubilizing bacteria: observations on barley. Plant Nano Biol. 9, 100091. https://doi.org/10.1016/j.plana.2024.100091.

Poosakkannu, A., Nissinen, R., Kytöviita, M.M., 2015. Culturable endophytic microbial communities in the circumpolar grass, *Deschampsia flexuosa* in a sub-Arctic inland primary succession are habitat and growth stage specific. Environ. Microbiol. Rep. 7, 111–122. https://doi.org/10.1111/1758-2229.12195.

Priyam, A., Das, R.K., Schultz, A., Singh, P.P., 2019. A new method for biological synthesis of agriculturally relevant nanohydroxyapatite with elucidated effects on soil bacteria. Sci. Rep. UK 9, 15083. https://doi.org/10.1038/s41598-019-51514-0.

Raymond, N.S., Gómez-Muñoz, B., van der Bom, F.J., Nybroe, O., Jensen, L.S., Müller-Stöver, D.S., Oberson, A., Richardson, A.E., 2021. Phosphate-solubilizing microorganisms for improved crop productivity: a critical assessment. New Phytol. 229, 1268–1277. https://doi.org/10.1111/nph.16924.

Reynolds, C.S., Davies, P.S., 2001. Sources and bioavailability of phosphorus fractions in freshwaters: a British perspective. Biol. Rev. 76, 27–64. https://doi.org/10.1017/S1464793100005625.

Roberts, T.L., Johnston, A.E., 2015. Phosphorus use efficiency and management in agriculture. Resour. Conserv. Recycl. 105, 275–281. https://doi.org/10.1016/j.resconrec.2015.09.013.

Rocha, I., Ma, Y., Souza-Alonso, P., Vosátka, M., Freitas, H., Oliveira, R.S., 2019. Seed coating: a tool for delivering beneficial microbes to agricultural crops. Front. Plant Sci. 10, 1357. https://doi.org/10.3389/fpls.2019.01357.

Rodriguez, H., Fraga, R., 1999. Phosphate solubilizing bacteria and their role in plant growth promotion. Biotechnol. Adv. 17, 319–339. https://doi.org/10.3389/fpls.2019.01357.

Rosier, A., Medeiros, F.H., Bais, H.P., 2018. Defining plant growth promoting rhizobacteria molecular and biochemical networks in beneficial plant-microbe interactions. Plant Soil 428, 35–55. https://doi.org/10.1007/s11104-018-3679-5.

Santana, C.A., Piccirillo, C., Pereira, S.I.A., Pullar, R.C., Lima, S.M., Castro, P.M.L., 2019. Employment of phosphate solubilizing bacteria on fish scales-turning food waste into an available phosphorus source. J. Environ. Chem. Eng. 7, 103403. https://doi.org/10.1016/j.jece.2019.103403.

Sasson, Y., Levy-Ruso, G., Toledano, O., Ishaaya, I., 2007. Nanosuspensions: emerging novel agrochemical formulations. In: Insecticides Design Using Advanced Technologies. Springer, Berlin, Germany, pp. 1–39.

Sawers, R.J., Svane, S.F., Quan, C., Grønlund, M., Wozniak, B., Gebreselassie, M., González Muñoz, E., Chávez Montes, E.A., Baxter, I., Goudet, J., Jakobsen, I., Paszkowski, U., 2017. Phosphorus acquisition efficiency in arbuscular mycorrhizal maize is correlated with the abundance of root-external hyphae and the accumulation of transcripts encoding PHT1 phosphate transporters. New Phytol. 214, 632–643. https://doi.org/10.1111/nph.14403.

Saxena, A.K., Kumar, M., Chakdar, H., Anuroopa, N., Bagyaraj, D.J., 2020. *Bacillus* species in soil as a natural resource for plant health and nutrition. J. Appl. Microbiol. 128, 1583–1594. https://doi.org/10.1111/jam.14506.

Schindler, D.W., Kalff, J., Welch, H.E., Brunskill, G.J., Kling, H., Kritsch, N., 1974. Eutrophication in the High Arctic—Meretta Lake, Cornwallis Island (75 N Lat.). J. Fish. Board Can. 31, 647–662. https://doi.org/10.1139/f74-096.

Sessitsch, A., Coenye, T., Sturz, A.V., Vandamme, P., Barka, E.A., Salles, J.F., Van Elsas, J.D., Faure, D., Reiter, B., Glick, B.R., Wang-Pruski, G., Nowak, J., 2005. *Burkholderia phytofirmans* sp. nov., a novel plant-associated bacterium with plant-beneficial properties. Int. J. Syst. Evol. Microbiol. 55, 1187–1192. https://doi.org/10.1099/ijs.0.63149-0.

Sharma, R., Chandel, S., Chauhan, A., Shirkot, C.K., 2015. Enhanced phosphorus solubilization by *Bacillus licheniformis* CKA1 using central composite design and response surface methodology. J. Pure Appl. Microbiol. 3131–3141.

Sharpley, A.N., Kleinman, P., McDowell, R., 2001. Innovative management of agricultural phosphorus to protect soil and water resources. Commun. Soil Sci. Plant Anal. 32, 1071–1100. https://doi.org/10.1081/CSS-100104104.

Shen, J., Yuan, L., Zhang, J., Li, H., Bai, Z., Chen, X., Zhang, W., Zhang, F., 2011. Phosphorus dynamics: from soil to plant. Plant Physiol. 156, 997–1005. https://doi.org/10.1104/pp.111.175232.

Shilev, S., Babrikova, I., Babrikov, T., 2020. Consortium of plant growth-promoting bacteria improves spinach (*Spinacea oleracea* L.) growth under heavy metal stress conditions. J. Chem. Technol. Biotechnol. 95, 932–939. https://doi.org/10.1002/jctb.6077.

Smith, F.W., Mudge, S.R., Rae, A.L., Glassop, D., 2003. Phosphate transport in plants. Plant Soil 248, 71–83. https://doi.org/10.1023/A:1022376332180.

Sonmez, O., Pierzynski, G.M., 2017. Changes in soil phosphorus fractions resulting from crop residue removal and phosphorus fertilizer. Commun. Soil Sci. Plant Anal. 48, 929–935. https://doi.org/10.1080/00103624.2017.1323094.

Srivastava, S., Srivastava, S., 2020. Prescience of endogenous regulation in Arabidopsis thaliana by *Pseudomonas putida* MTCC 5279 under phosphate starved salinity stress condition. Sci. Rep. UK 10, 5855. https://doi.org/10.1038/s41598-020-62725-1.

Swaney, D.P., Howarth, R.W., 2019. Phosphorus use efficiency and crop production: patterns of regional variation in the United States, 1987–2012. Sci. Total Environ. 685, 174–188. https://doi.org/10.1016/j.scitotenv.2019.05.228.

Taskin, H., Gunes, A., 2023. Synthetic nano-hydroxyapatite as an alternative phosphorus source for wheat grown under field conditions. J. Plant Nutr. 46, 3653–3666. https://doi.org/10.1080/01904167.2023.2210157.

Teixeira, M.A.C., Piccirillo, C., Tobaldi, D.M., Pullar, R.C., Labrincha, J.A., Ferreira, M.O., Castro, P.M.L., Pintado, M.M.E., 2017. Effect of preparation and processing conditions on UV-absorbing properties of hydroxyapatite-Fe_2O_3 sunscreen. Mater. Sci. Eng. 141-149. https://doi.org/10.1016/j.msec.2016.09.065.

Tian, H., Drijber, R.A., Li, X., Miller, D.N., Wienhold, B.J., 2013. Arbuscular mycorrhizal fungi differ in their ability to regulate the expression of phosphate transporters in maize (*Zea mays* L.). Mycorrhiza 23, 507–514. https://doi.org/10.1007/s00572-013-0491-1.

Tian, S., Xu, Y., Zhong, Y., Qiao, Y., Wang, D., Wu, L., Yang, X., Yang, M., Wu, Z., 2024. Exploring the organic acid Secretion pathway and potassium solubilization ability of *Pantoea vagans* ZHS-1 for enhanced rice growth. Plants 13, 1945. https://doi.org/10.3390/plants13141945.

Vadhel, A., Kumar, A., Bashir, S., Malik, T., Mohan, A., 2023. Synergistic and non-synergistic impact of HAP-based nano fertilizer and PGPR for improved nutrient utilization and metabolite variation in hemp crops. Environ. Sci. Nano 10, 3101–3110. https://doi.org/10.1039/D3EN00380A.

Van Vuuren, D.P., Bouwman, A.F., Beusen, A.H., 2010. Phosphorus demand for the 1970-2100 period: a scenario analysis of resource depletion. Glob. Environ. Chang. 20, 428–439. https://doi.org/10.1016/j.gloenvcha.2010.04.004.

Veneklaas, E.J., Lambers, H., Bragg, J., Finnegan, P.M., Lovelock, C.E., Plaxton, W.C., Price, C.A., Scheible, W.R., Shane, M.W., White, P.J., Raven, J.A., 2012. Opportunities for improving phosphorus-use efficiency in crop plants. New Phytol. 195, 306–320. https://doi.org/10.1111/j.14698137.2012.04190.x.

Vilgalys, R., Hester, M., 1990. Rapid genetic identification and mapping of enzymatically amplified ribosomal DNA from several *Cryptococcus* species. J. Bacteriol. 172, 4238–4246. https://doi.org/10.1128/jb.172.8.4238-4246.1990.

Vio, S.A., García, S.S., Casajus, V., Arango, J.S., Galar, M.L., Bernabeu, P.R., Luna, M.F., 2020. *Paraburkholderia*. In: Beneficial Microbes in Agro-ecology. Academic Press, Elsevier, Amsterdam, The Netherlands, pp. 271–311.

Wang, D., Xie, Y., Jaisi, D.P., Jin, Y., 2016. Effects of low-molecular-weight organic acids on the dissolution of hydroxyapatite nanoparticles. Environ. Sci. Nano 3, 768–777. https://doi.org/10.1039/C6EN00085A.

Wang, D., Lv, S., Jiang, P., Li, Y., 2017. Roles, regulation, and agricultural application of plant phosphate transporters. Front. Plant Sci. 8, 817. https://doi.org/10.3389/fpls.2017.00817.

Wang, Y., Cui, Y., Wang, K., He, X., Dong, Y., Li, S., Wang, Y., Yang, H., Chen, X., Zhang, W., 2023. The agronomic and environmental assessment of soil phosphorus levels for crop production: a meta-analysis. Agron. Sustain. Dev. 43, 35. https://doi.org/10.1007/s13593-023-00887-8.

Wickham, H., Wickham, H., 2016. Getting Started With ggplot2. ggplot2: Elegant Graphics for Data Analysis, pp. 11–31.

Xiong, L., Wang, P., Hunter, M.N., Kopittke, P.M., 2018a. Bioavailability and movement of hydroxyapatite nanoparticles (HA-NPs) applied as a phosphorus fertiliser in soils. Environ. Sci. Nano 5, 2888–2898. https://doi.org/10.1039/C8EN00751A.

Xiong, L., Wang, P., Kopittke, P.M., 2018b. Tailoring hydroxyapatite nanoparticles to increase their efficiency as phosphorus fertilisers in soils. Geoderma 323, 116–125.

Yasmeen, T., Arif, M.S., Shahzad, S.M., Riaz, M., Tufail, M.A., Mubarik, M.S., Ahmad, A., Ali, S., Albasher, G., Shakoor, A., 2022. Abandoned agriculture soil can be recultivated by promoting biological phosphorus fertility when amended with nano-rock phosphate and suitable bacterial inoculant. Ecotox. Environ. Safe. 234, 113385. https://doi.org/10.1016/j.ecoenv.2022.113385.

Zhang, L., Tan, C., Li, W., Lin, L., Liao, T., Fan, X., Peng, H., An, Q., Liang, Y., 2024. Phosphorus, potassium, and silicon-solubilizing bacteria from forest soils can mobilize soil minerals to promote the growth of rice (*Oryza sativa* L.). Chem. Biol. Technol. Agric. 11, 103. https://doi.org/10.1186/s40538-024-00622-9.

Zhang, W., Gong, J., Zhang, Z., Song, L., Lambers, H., Zhang, S., Dong, J., Dong, X., Hu, Y., 2023. Soil phosphorus availability alters the correlations between root phosphorus-uptake rates and net photosynthesis of dominant C_3 and C_4 species in a typical temperate grassland of Northern China. New Phytol. 240, 157–172. https://doi.org/10.1111/nph.19167.

Zhu, G., Sun, Y., Shakoor, N., Zhao, W., Wang, Q., Wang, Q., Wang, Q., Imran, A., Li, M., Li, Y., Jiang, Y., Adeel, M., Rui, Y., 2023. Phosphorus-based nanomaterials as a potential phosphate fertilizer for sustainable agricultural development. Plant Physiol. Biochem. 205, 108172. https://doi.org/10.1016/j.plaphy.2023.108172.